

The deep structure of the Australian continent from surface wave tomography

Frederik J. Simons^{*}, Alet Zielhuis, Rob D. van der Hilst

Department of Earth, Atmospheric and Planetary Sciences, Massachusetts Institute of Technology, Rm 54-517A, Cambridge, MA 02139, USA

Received 16 April 1999; received in revised form 10 May 1999; accepted 11 May 1999

Abstract

We present a new model of 3-D variations of shear wave speed in the Australian upper mantle, obtained from the dispersion of fundamental and higher-mode surface waves. We used nearly 1600 Rayleigh wave data from the portable arrays of the SKIPPY project and from permanent stations (from AGSO, IRIS and GEOSCOPE). AGSO data have not been used before and provide better data coverage of the Archean cratons in western Australia. Compared to previous studies we improved the vertical parameterization, the weighting scheme that accounts for variations in data quality and reduced the influence of epicenter mislocation on velocity structure. The dense sampling by seismic waves provides for unprecedented resolution of continental structure, but the wave speed beneath westernmost Australia is not well constrained. Global compilations of geological and seismological data (using regionalizations based on tectonic behavior or crustal age) suggest a correlation between crustal age and the thickness and composition of the continental lithosphere. However, the age and the tectonic history of crustal elements vary on wavelengths much smaller than have been resolved with global seismological studies. Using our regional upper mantle model we investigate how the seismic signature of tectonic units changes with increasing depth. At large wavelengths, and to a depth of about 200 km, the inferred velocity anomalies corroborate the global pattern and display a progression of wave speed with crustal age: slow wave propagation prevails beneath the Paleozoic fold belts in eastern Australia and wave speeds increase westward across the Proterozoic and reach a maximum in the Archean cratons. The high wave speeds associated with Precambrian shields extend beyond the Tasman Line, which marks the eastern limit of Proterozoic outcrop. This suggests that parts of the Paleozoic fold belts are underlain by Proterozoic lithosphere. We also infer that the North Australia craton extends off-shore into Papua New Guinea and beneath the Indian Ocean. For depths in excess of 200 km a regionalization with smaller units reveals that some tectonic subregions of Proterozoic age are marked by pronounced velocity highs to depths exceeding 300 km, but others do not and, surprisingly, the Archean units do not seem to be marked by such a thick high wave speed structure either. The Precambrian cratons that lack a thick high wave speed “keel” are located near passive margins, suggesting that convective processes associated with continental break-up may have destroyed a once present tectosphere. Our study suggests that deep lithospheric structure varies as much within domains of similar crustal age as between units of different ages, which hampers attempts to find a unifying relationship between seismic signature and lithospheric age. © 1999 Elsevier Science B.V. All rights reserved.

Keywords: Continental lithosphere; Rayleigh wave; SKIPPY project; Broadband data; Waveform tomography; Australia

^{*} Corresponding author. Tel.: +1-617-253-0741; fax: +1-617-258-9697; E-mail: fjsimons@mit.edu

1. Introduction

The inference that continental geotherms in the Archean were not much different from the averages seen today, despite pervasively (200–300°) hotter mantle temperatures, has been supported (but also refuted, e.g., Strong and Stevens, 1974) by both observations (Burke and Kind, 1978; Boyd and Gurney, 1986; Boyd, 1989) and numerical simulations (Richter, 1984, 1985; Lenardic, 1998) (see also Jaupart and Mareschal, 1999, and Nyblade, 1999, this volume). Combined with experimental data on diamond stability in the mantle, the age of the continental lithospheric mantle (CLM) inferred from diamond inclusions (Richardson et al., 1984) and Re-OS dating of mantle xenoliths (Pearson et al., 1995; Pearson, 1999, this volume), and the correlation between composition of continental mantle and the age of the overlying crust (Griffin et al., 1998) this suggests the presence of a thick (≥ 175 km) Archean and Early-Proterozoic subcontinental lithosphere that has stabilized shortly after being formed and has remained coupled to the crust ever since. This “cold” lithosphere, with geothermal gradients generally less than 23° km^{-1} (Burke and Kind, 1978), must have been stabilized against convective disruption by its composition and its rheological properties (Jordan, 1988; Richter, 1988; De Smet et al., 1999, this volume; Shapiro et al., 1999a, this volume).

Cooling of the lithosphere provides a satisfactory explanation for the geophysical signature (e.g., gravity, bathymetry, seismic properties) of oceanic plates (Sclater et al., 1981), but the large CLM thickness inferred from seismic imaging cannot be explained by cooling alone. If a cold, negatively buoyant continental lithosphere is stabilized by rheology (that is, the strength of the plate) the thermally induced density contrasts would produce anomalies in the long-wavelength gravity field and geoid, which are not observed (Kaula, 1967; Jordan, 1975b, 1978; Shapiro et al., 1999b, this volume). Considering geological, geochemical, and geophysical evidence, Jordan (1975b, 1978) postulated a mechanism for producing a petrologically distinct chemical boundary layer under the cratonic parts of the continents. In his isopycnic model the negative buoyancy of cold lithosphere is compensated by positive compositional buoyancy. Neutrally buoyant and probably more viscous than

the surrounding mantle, this “keel” of depleted, refractory continental mantle, or tectosphere, is thought to remain coupled to the crust for billions of years and thus plays a crucial role in regulating continental development and stability (Jordan, 1981a, 1988). The presence of such “keels” has been corroborated by seismological studies that reveal a (300–500 km) thick, anomalously fast lithosphere under some of the oldest parts of the continents (Jordan, 1975a; Sipkin and Jordan, 1975, 1976; Woodhouse and Dziewonski, 1984; Su et al., 1994; Masters et al., 1996; Ekström et al., 1997; van der Lee and Nolet, 1997b). To first order this relationship seems to hold globally (Okal, 1977; Jordan, 1981b; Polet and Anderson, 1995), but, as we show in this study, significant departures may occur on smaller length scales.

The lateral variation in upper mantle structure, such as the differences between oceanic and continental regions and between stable or tectonically active domains, can be studied with a variety of seismic imaging techniques. The type of data used depend on the specific research objectives. Elsewhere in this volume, Bostock (1999) reviews techniques used for high-resolution imaging of the crust and lithospheric mantle with phase conversions and scattering of seismic body waves. Here we consider variations in elastic properties on a larger scale than considered by Bostock; these can be constrained by a variety of methods and data, for example dispersion curves of fundamental-mode surface waves (Toksöz and Anderson, 1966; Priestley, 1999, this volume), the dispersion of singlets in the eigenfrequency multiplets of fundamental spheroidal and toroidal modes (Dahlen, 1976), vertical delay times of (multiply) reflected body wave phases (Sipkin and Jordan, 1975, 1976), and higher mode phase and group velocities (Cara, 1979). With the advent of different methods of surface-wave tomography (Woodhouse and Dziewonski, 1984; Nolet, 1990; Trampert and Woodhouse, 1995, 1996; Ekström et al., 1997) direct images have been made of the aspherical structure of the upper mantle. Typically, the horizontally propagating surface waves provide better radial resolution than vertically incident body waves, especially when higher modes are included in the analysis. Body waves potentially provide better lateral resolution of lithospheric structure. In general, global data sets

resolve structure on the scale of sub-continental age provinces. For example, the two-fold division of Australia into a Phanerozoic and Precambrian part is resolved in the global models (Ekström et al., 1997), but these do not constrain variations in structure over distances less than about 1000 km (Laske and Masters, 1996). Regional studies can provide better horizontal resolution, in particular if additional data from regional seismometer networks are available.

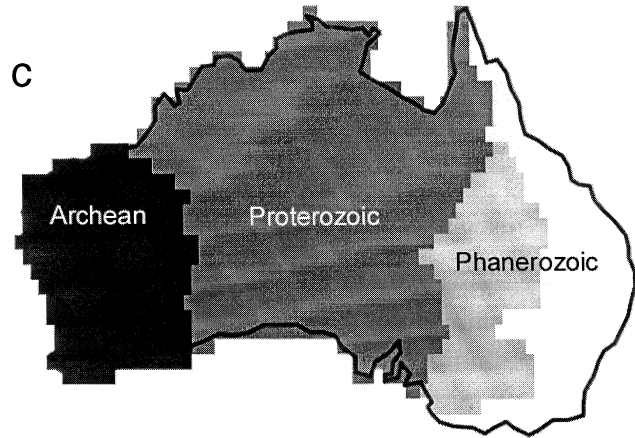
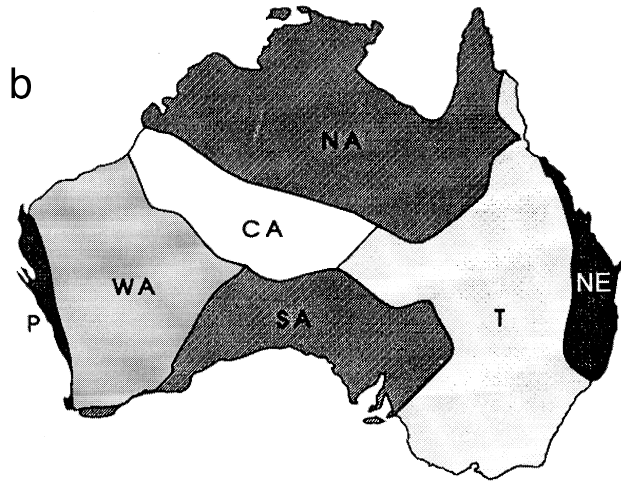
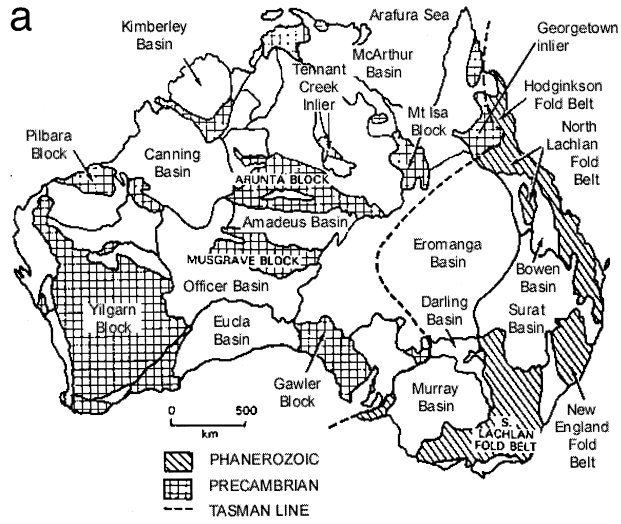
Australia is well suited to investigate deep continental structure. The makeup of the continent is extremely varied (Fig. 1). Based on outcrop, continental Australia can be divided in a western, central, and eastern domain (see Fig. 1c) but smaller-scale units have been identified as well (see Fig. 1a, b). The western third of the continent comprises granites and greenstones of the Pilbara and Yilgarn blocks, which formed in the Archean (3500 and 3100 Ma, respectively) and have been stable since at least 2300 Ma (Plumb, 1979). There is little or no Phanerozoic cover of these cratonic units. Central Australia consists of a series of intracratonic Late-Proterozoic–Early-Paleozoic basins separated by fault-bounded blocks exposing Mid-Proterozoic basement rocks (Lambeck, 1983). The Tasman Line — first drawn by Hill in 1951 (Veevers, 1984) but different interpretations exist — separates this Precambrian outcrop from exposed Phanerozoic formations in the east. Its definition is based largely on surface geology and, in regions of limited exposure (such as across the Eromanga basin), on lineations in gravity and magnetic anomaly maps (Murray et al., 1989; Wellman, 1998). Moreover, the continent is favorably located with respect to zones of active seismicity (Fig. 2), which provide ample sources for seismic tomographic imaging, and the SKIPPY seismometry project (van der Hilst et al., 1994) has provided data coverage that allows surface wave tomography with unprecedented resolution.

In this paper we briefly describe the tomographic technique that we have used to determine lateral variations in shear wave speed in the Australian mantle and discuss the relationship between the thickness of the high wave speed lithosphere and variations in crustal age. We present our model both in terms of the inversion results and as wave speed averages over well-defined geotectonic regions. Using regionalizations at different spatial scales we

show that the deep structure of the Australian continent varies significantly, not only across the large-scale tectonic units but also within domains of roughly the same age. These observations are important for our understanding of the Australian continent but also have ramifications for studies of deep continental structure and evolution on the basis of global regionalizations of crustal age and tectonic history.

2. Imaging with seismic waves: seismic tomography

Tomography is a technique for reconstructing a function (“the unknowns”, or “the model”) from projections (“the data”) along a set of curves. This relationship is often expressed as an integral over a certain volume V , $\int_V g_i(\mathbf{r})\delta x(\mathbf{r})d\mathbf{r} = b_i$, with $g_i(\mathbf{r})$ the Fréchet derivative (or sensitivity kernel) describing the functional dependence of the measurements b_i on the model perturbations $\delta x(\mathbf{r})$ (or in linearized form as a system of normal equations $\mathbf{Ax} = \mathbf{b}$, with \mathbf{A} the sensitivity matrix containing the appropriate Fréchet derivatives and \mathbf{x} and \mathbf{b} the model and data vector, respectively). If the medium under study is the human body, then the function might be the density of organ tissue, and the data used to constrain it might be the intensity of transmitted X-rays (the principle behind many kinds of medical tomography (Herman, 1979)). For imaging the Earth, one uses seismic waves, which are affected by anomalous structure, so that the phase arrival time, amplitude, or entire waveform differ from the ones expected in a spherical reference Earth model. Such differences are then interpreted in terms of velocity and attenuation variations of seismic waves within the Earth. A major complication is that the sources (earthquakes or man-made explosion) and receivers (seismometers) are distributed very unevenly over the surface of the Earth so that some regions are constrained by many data whereas others are not sampled at all. This renders the tomographic problem underdetermined (that is, not all unknowns can be determined independently) and the solution is non-unique. Out of a large number of solutions we choose a solution by minimizing a penalty function,



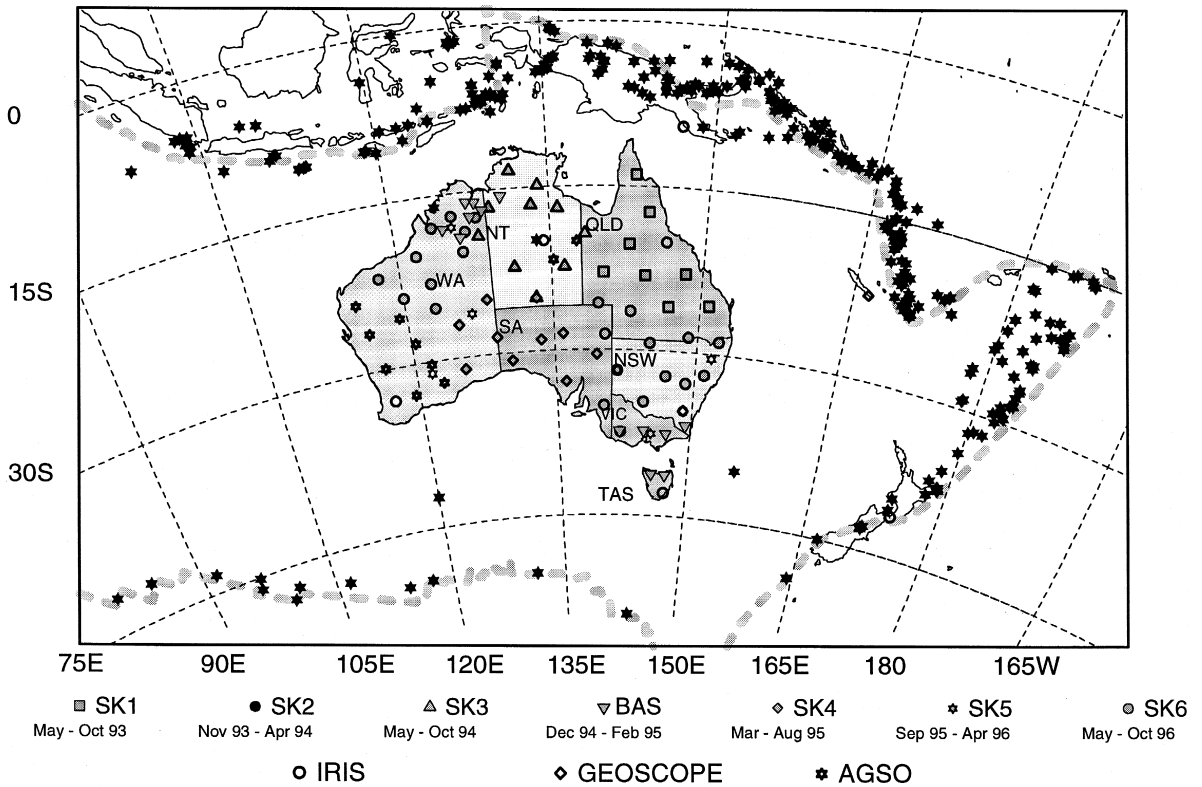


Fig. 2. Locations of the SKIPPY, IRIS, GEOSCOPE, and AGSO stations used in this study. The solid stars depict epicenters of all earthquakes (source: Engdahl et al., 1998) for which data were used in this study ($N = 336$). Abbreviations used: QLD: Queensland, NSW: New South Wales, VIC = Victoria, SA = South Australia, TAS = Tasmania, NT = Northern Territory, WA = West Australia. Gray dashed lines depict plate boundaries.

which typically includes regularization terms (also known as damping) and accounts for a priori information.

Different kinds of seismic tomography exist (see, for example, the overview by Nolet (1987)). The data that can be used differ in frequency content and in the way they sample Earth's interior (see Fig. 3). Body-wave tomography often makes use of travel-

time perturbations from reference times. With surface waves, which typically have lower frequencies than body waves, the principle is the same, but they sample the Earth in a different manner. Rather than having their sensitivity to Earth structure concentrated along a ray path (such as in Fig. 3b) this sensitivity is given by a frequency-dependent kernel (Fig. 4). Frequency is a proxy for depth; the higher

Fig. 1. The geology of Australia at different scales and with different definitions of the units. (a) Most detailed representation considered in this paper. The dashed line is the Tasman Line, which divides the Precambrian western Australia from Phanerozoic eastern Australia (from Zuber et al., 1989). (b) Australian crustal elements, representing continent-scale groups of geophysical domains (from Wellman, 1998). CA, Central Australia; NA, Northern Australia; P: Pinjarra; WA, Western Australia; SA, South Australia; T, Tasman; NE, New England. (c) A coarse, fourfold regionalization of the Australian continent based on crustal age. The crustal age decreases from Archean in the westernmost part, to predominantly Proterozoic in the central part, and Phanerozoic to the right of the Tasman line.

the frequency of the waves the more their sensitivity shifts to shallower depths. For a given frequency, the fundamental mode surface waves (Fig. 4a) sample shallower structure than the higher modes (Fig. 4b), and inclusion of the latter thus provides for increased depth resolution.

3. Partitioned waveform inversion (PWI)

The interpretation of waveforms in terms of aspherical variations in Earth's structure is often partitioned into (1) a non-linear waveform inversion that, for each record, seeks to determine the 1D structure

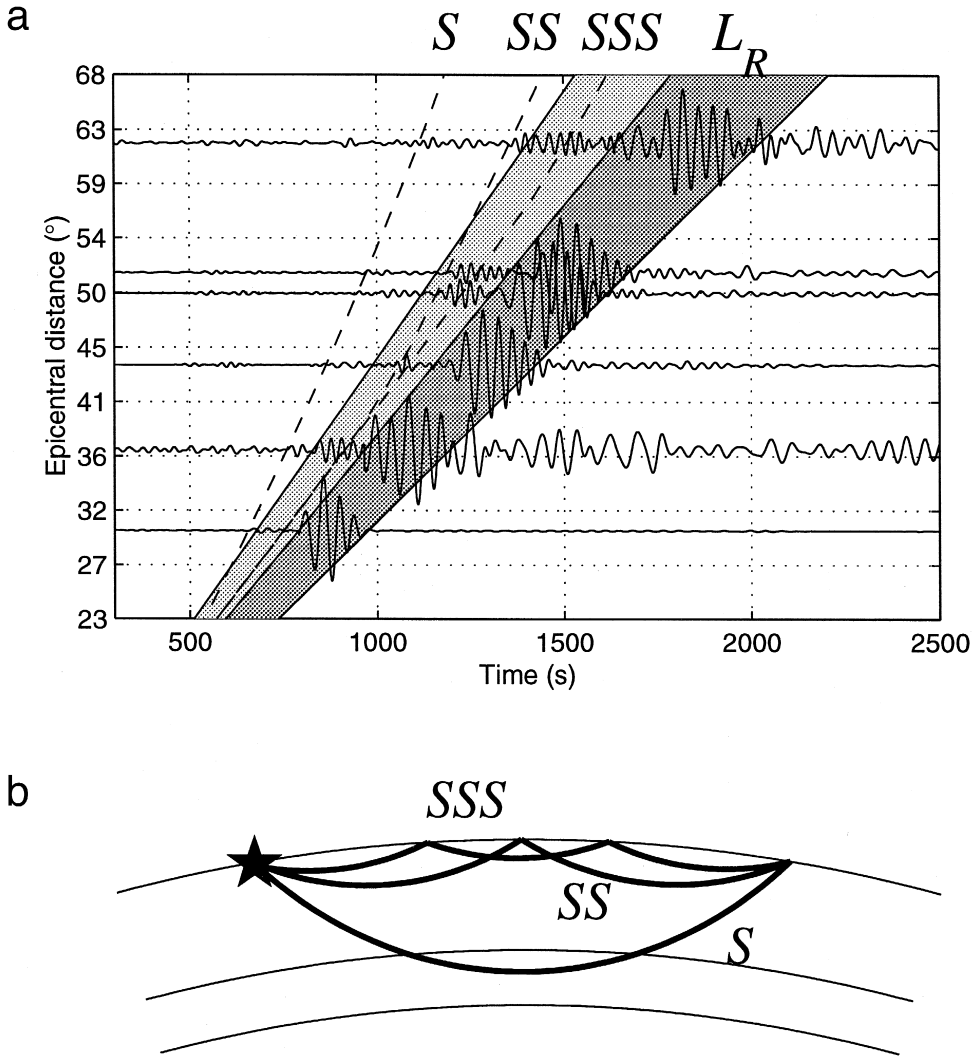


Fig. 3. Body and surface-wave phases. (a) Composite record section of vertical-component seismograms arranged in order of increasing epicentral distance to two different earthquakes. The dashed lines represent the arrival times of the body-wave phases S , SS and SSS calculated from the *ak135* wave speed model (Kennett et al., 1995). The Rayleigh-wave surface wave L_R can be thought of as a limiting case of multiple reflections propagating across the surface. The solid lines and shaded areas indicate two group velocity windows. The first window, defined between 4.9 and 4.2 km s^{-1} selects phases sampling the upper-mantle (the “higher-mode window”). The second window, between 4.2 and 3.4 km s^{-1} selects fundamental-mode surface waves. We note that for each record the precise windows are set manually upon visual inspection of the waveforms. Seismograms have been filtered between 10 and 45 mHz for the higher modes, and between 10 and 25 mHz for the fundamental modes. (b) Ray geometry in the upper mantle of the body-wave phase shown in (a).

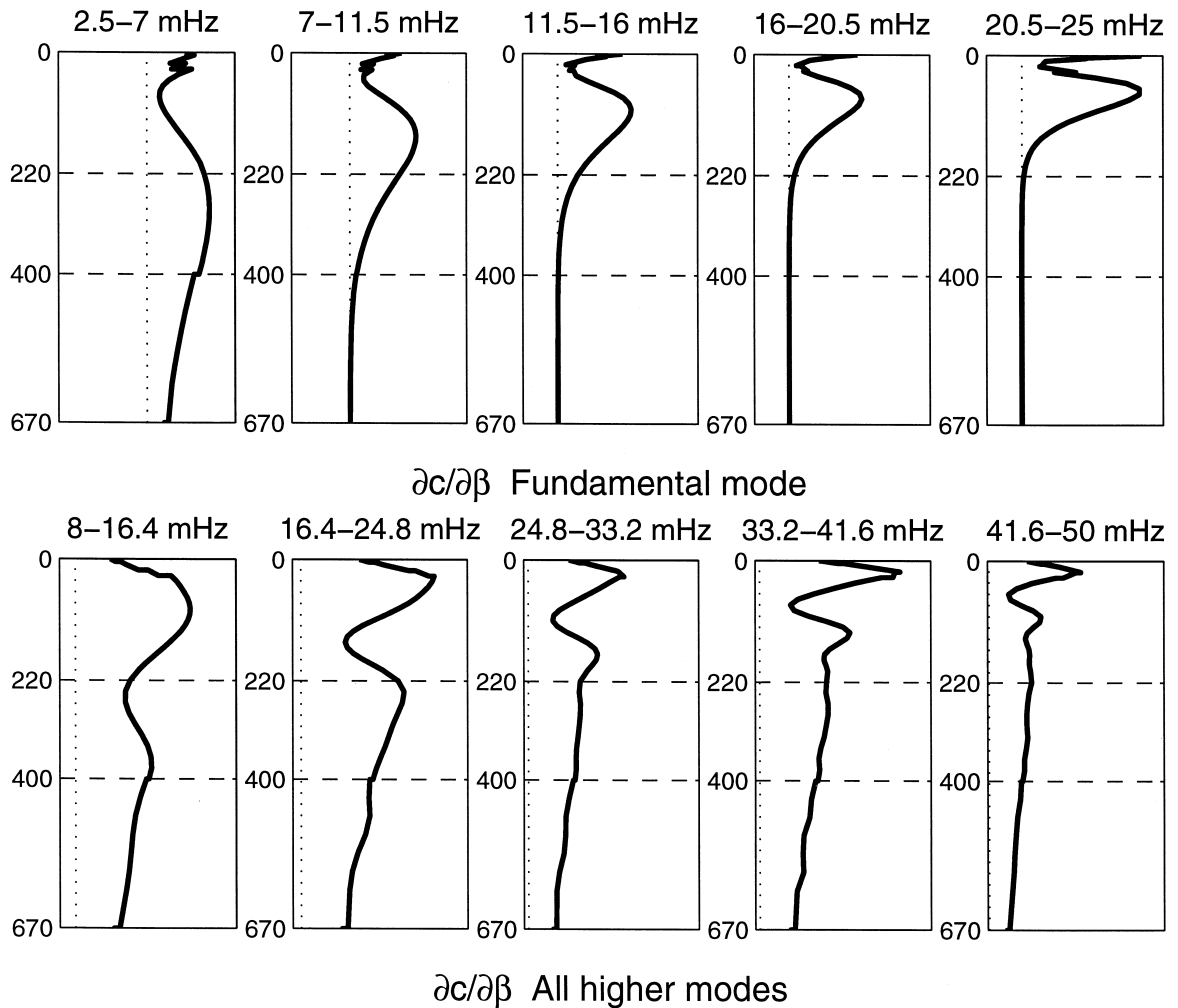


Fig. 4. Sensitivity (Fréchet) kernels for surface wave propagation. The kernels represent $\partial c/\partial\beta(r)$, i.e., the sensitivity of the phase velocity c of a particular set of surface wave modes to a perturbation of the shear-wave speed β at a particular depth. (Top) Fundamental mode. (Bottom) Higher modes. Surface-wave studies done with fundamental modes are mostly sensitive to shallow structure, while most of the sensitivity at depth is due to the higher modes.

between source and receiver (see Section 3.1) and (2) a geometrical, linear tomographic inversion which combines the individual path constraints into a 3D model for Earth structure (see Section 3.2). Partitioned Waveform Inversion (PWI), developed by Nolet (1990), has previously been used to study the upper mantle beneath Europe (Nolet, 1990; Zielhuis and Nolet, 1994a,b), South Africa (Cichowicz and Green, 1992), North America (van der Lee and Nolet, 1997a,b), and Australia (Zielhuis and van der

Hilst, 1996). Here we review some basic aspects of the technique; for more complete descriptions we refer to Nolet et al. (1986), Nolet (1990), and Zielhuis and Nolet (1994a).

3.1. Waveform inversion for path-averaged structure

In the first step of PWI individual seismograms are analyzed and, within the restrictions discussed below, inverted for shear velocity variations with

depth, $\delta\beta(r)$ (with r radius), averaged along the source–receiver path. This involves the matching of observed waveforms with theoretical (synthetic) seismograms, which are computed as a sum of surface-wave modes using the JWKB approximation (Woodhouse, 1974). The waveform synthesis requires information about the earthquake focal mechanisms, which is obtained from the Harvard Centroid Moment Tensor (CMT) catalog (Dziewonski et al., 1981) and the National Earthquake Information Center (NEIC) (Sipkin, 1994).

The JWKB formalism assumes that lateral heterogeneity is sufficiently smooth compared to the wavelength of the seismic waves used, which imposes a lower limit for frequency. For our application, with perturbation scale lengths typically greater than ~ 400 km, epicentral distances ranging from 1000 to 4000 km, and a typical phase speed of about 4.5 km s^{-1} , a lower frequency limit of not much less than 10 mHz is predicted on theoretical grounds (Kennett, 1995; Wang and Dahlen, 1995; Dahlen and Tromp, 1998). In practice this criterion can be relaxed a bit and for the fundamental modes we consider a lower limit of 5 mHz (although most data are for frequencies higher than 8 mHz). The path-average approximation also implies an upper-frequency limit, both for the fundamental mode and the overtones, because cross-branch coupling between modes, as would arise from lateral heterogeneity (Kennett, 1984; Li and Tanimoto, 1993; Marquering and Snieder, 1995) and which brings out the ray character of the higher modes, such as *SS*, is not accounted for. The detrimental effects of ignoring mode coupling are aggravated with increasing frequency. However, Marquering et al. (1996) and Marquering and Snieder (1996) have demonstrated that if data coverage is dense the results will be little changed by the adoption of mode coupling techniques in the inversion. Moreover, the largest differences would occur outside the depth range that is also constrained by the horizontally propagating fundamental modes; therefore, we only discuss structure to a depth of 400 km. (We note that structure beneath stations or events that is not well sampled by rays from different directions, such as on the edge of the model, may exhibit spurious vertical structure resulting from the one-dimensionality of the kernels. This may be the case for the deep fast anomaly beneath the NWA0 station at Narrogin,

West Australia.) At high frequencies the fundamental-mode Rayleigh waves become sensitive to steep gradients in shallow structure (Fig. 4), such as at the transition from oceanic to continental crust, which can severely distort the waveforms. Along with low-passing the data, we minimized such effects by accounting for variations in crustal thickness within the region under study on the basis of crustal thickness information from converted phases recorded at the SKIPPY stations (Shibutani et al., 1996; Clitheroe et al., submitted).

Kennett (1995) and Kennett and Nolet (1990) conclude that with an upper frequency limit of 20 mHz for the fundamental mode and 50 mHz for the higher modes the surface-mode summation used in PWI provides a representation of the seismic wave field that is adequate for our purposes. Because the admissible frequency limits differ we use group velocity windows to isolate the fundamental and higher mode part of the records so that we can analyze them within the frequency bands discussed above (see also Fig. 3).

An example of waveform fits is given in Fig. 5. The wave trains for the fundamental and higher modes have been normalized to unit amplitude. Both sections of the seismogram are fitted separately within the applicable frequency band. The initial fits depict the difference between the observed data (thick solid lines) and the synthetic records (thin lines) produced from a reference model. For this event in Southern Sumatra the fundamental-mode Rayleigh waves arrive earlier than predicted from the average Earth for all stations considered, suggesting relatively fast wave propagation across the western and central part of the continent. But at some stations the mismatch is larger than at others; compare, for instance, the records of ARMA (Armidale, New South Wales) and CTA (or CTAO, Charters Towers, Queensland). These differences are indicative of lateral variations in wave speed (for these earthquakes the data indicate that the average wave speed along the path to ARMA is faster than along the one to CTA). For the same stations, the difference between the observed and synthesized overtones are smaller than for the fundamental mode, suggesting that the wave speed variations in the deep part of the model are smaller than in the shallow part. The bottom panel of Fig. 5 shows the excellent (final) fit of the

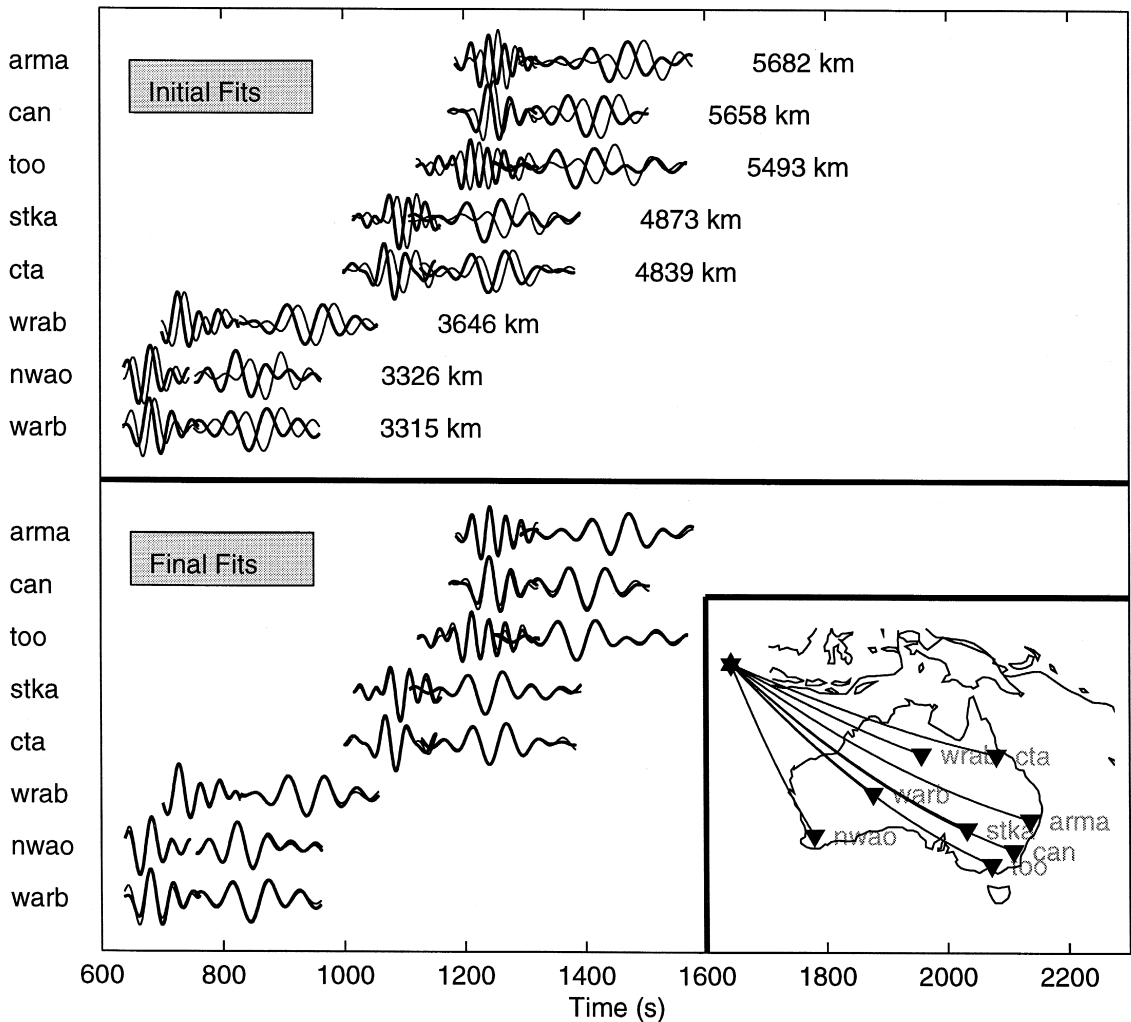


Fig. 5. Waveform fitting. Observed data are plotted as thick solid lines, predictions are depicted with thin lines. Seismograms are for a Mb 5.8 event in Southern Sumatra, at (103.9°E, 5.7°S), located at 56 km depth. Great circle paths to the stations are plotted in the inset. “Initial fits” are predictions made by surface-wave summation, using an assumed reference model. “Final fits” are obtained by the nonlinear inversion procedure described in Nolet et al. (1986) (see text).

waveforms, both for the higher-frequency overtones as well as for the lower-frequency fundamental modes.

3.2. Tomographic inversion for 3D structure

Once the path-average of the variation of wave speed with depth ($\delta\beta(r)$) is determined for each source–receiver combination these 1D profiles are used as observations in a tomographic inversion for

3D variations in shear wave speed ($\delta\beta(r, \theta, \varphi)$, with r radius, θ colatitude, and φ longitude). This linear tomographic inversion may be performed by a variety of methods, such as the ones described by Nolet (1990), Zielhuis (1992), Zielhuis and Nolet (1994b), or van der Lee and Nolet (1997b).

The tomographic problem is parameterized by means of local basis functions (equal-area blocks in latitude and longitude direction; and box-car and triangular basis functions for radius). The system of

equations is solved in a generalized least square sense, using the LSQR iterative algorithm (Paige and Saunders, 1982; Nolet, 1985). The damping applied is a combination of first-order gradient damping, which minimizes the differences in structure between adjacent cells, and norm damping, which produces a bias toward the reference model used. The model presented in this paper results from careful experimentation with all variables involved (damping, weights, cell size), and parameters such as variance reduction and retrieval of synthetic input models have been used as guidance. After 200 iterations of the LSQR inversion a variance reduction of about 90% was obtained. The reference model used for the 3D inversion has a crustal thickness of 30 km, which is a reasonable average for the region under study. For the mantle we used a modified PREM model (Dziewonski and Anderson, 1981), smoothly interpolated over the 220 km discontinuity (Zielhuis and Nolet, 1994b).

3.3. Differences with respect to previous studies of Australia

We have made several modifications to the methods by Zielhuis and Nolet (1994b), including a different form of weighting of the individual data fits, a parameterization with an increased number of basis functions in radial direction, and we added a parameter that can absorb effects of epicenter mislocation. The effects of these improvements are, however, subtle, and most of the differences with previous models (Zielhuis and van der Hilst, 1996; van der Hilst et al., 1998) can be attributed to the use of an expanded data set.

Firstly, we assign an uncertainty to the individual fits based on a weighted combination of the signal bandwidth, the length of the group velocity windows, the χ^2 -norm, and the zero-lag cross-correlation value of the synthetic and observed waveforms, as well as the ability to fit both the fundamental and higher mode data. The reciprocals of the uncertainties obtained were used to weight the data in the inversion. Secondly, like Zielhuis and Nolet (1994b) we used a combination of boxcar and triangular basis functions, but we have added additional node points in order to extract more information on deep structure from the large number of higher modes in our

data set. Thirdly, we have used the hypocenter locations from the global data file by Engdahl et al. (1998), but in this region source mislocations can be substantial owing to sparse station coverage of the southern hemisphere. A mislocation of 20 km, on an epicentral distance of 2000 km can cause a spurious wave speed anomaly of 1%. Without attempting a formal earthquake relocation we aimed to absorb such effects of source mislocation in a denuisancing parameter in the linear inversion for 3D structure. This has an effect similar to damping, and varying the degree of source relocation allows us to identify the structural features in our model that are required by the waveform data only.

4. Data used in this study

Between May 1993 and October 1996 the Australian National University operated the Skippy seismometry project (van der Hilst et al., 1994). This project involved 6 arrays of up to 12 portable broadband seismometers that together synthesized a nationwide array (Fig. 2) and was intended to exploit Australia's location with respect to regional seismicity and provide dense data coverage for a range of tomographic imaging techniques. The individual arrays were deployed for about 6 months at a time. Parts of the large set of surface wave data were used in previous studies (Zielhuis and van der Hilst, 1996; van der Hilst et al., 1998), which focused on central and eastern Australia because data coverage in the west was not satisfactory at the time. In addition to the data from the SKIPPY experiment we have used data from broadband permanent stations from the IRIS (Incorporated Research Institutions for Seismology), GEOSCOPE, and AGSO (Australian Geological Survey Organization). The ~ 1600 vertical-component seismograms from about 340 seismic events provide excellent data coverage (Fig. 6). Further improvements in the resolution, in particular of the western part of the continent, are still expected, given the continued monitoring of earthquake activity by AGSO.

We used the portion of the vertical-component seismogram from the arrival of direct *S* up to, and including, the arrival of the fundamental mode of the Rayleigh wave. This time window includes multiple

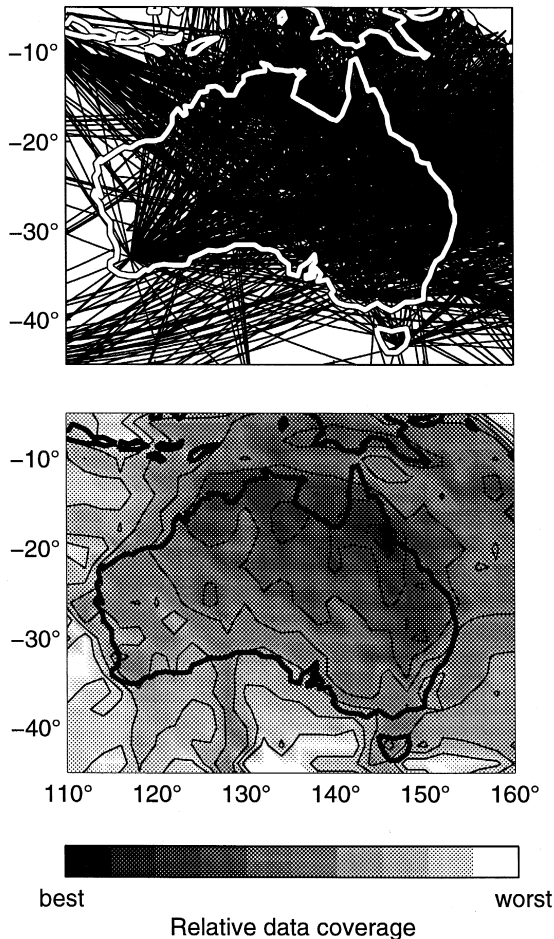


Fig. 6. (Top) Great-circle paths of the 1596 event-receiver combinations used in this study. (Bottom) Path coverage. Path lengths and variance of the directions of the rays crossing in $2^\circ \times 2^\circ$ cells, two indicators of tomographic quality, are combined and expressed on a relative scale (black indicates well sampled; white indicates no sampling).

body wave reflections at the free surface, such as *SS* and *SSS* (Fig. 3). The group velocity windows used for the isolation of the fundamental and higher modes are approximately 3.4–4.2 and 4.0–5.0 km s^{-1} , respectively, but for each individual record the exact limits are set after visual inspection. With this selection, the fundamental mode is truncated before the arrival of scattered and multipathed surface waves, and body waves with turning points in the deep mantle are excluded. For example, direct *S* is the first body wave phase considered at a distance of

2000 km, but at 4000 km this is *SS*, and at 6000 km *SSS*, etc. (Fig. 3). In recognition of the frequency limitations imposed by the approximations implicit in the method (see above), fundamental mode data were fit in the 5–25 mHz range and the higher modes were modeled within 8–50 mHz. About 40% of all seismograms contained higher-mode windows for which good fits could be obtained.

5. Results

Here we discuss briefly the spatial resolution and the general aspects of our model, compare our results to variations in shear wave speed as inferred from a global inversion, and describe in detail how the shear wave speed varies within several well-defined tectonic units that constitute the Australian continent.

5.1. Spatial resolution

Image quality does not only depend on the sheer number of data but also on the azimuthal distribution of the (crossing) paths (Aki and Richards, 1980; Menke, 1989; Lay and Wallace, 1995). For each cell, we added the variance of the directions (between 0 and π) of the rays (normalized from 0 to 1) to the normalized sum of the path lengths to provide a better measure of the quality of data coverage (Fig. 6). The data coverage is good throughout the Australian continent but degrades towards the southwest. Since all AGSO data have not yet been used we expect further improvements in this part of the continent.

In order to assess the reliability of the images we have performed test inversions with synthetic data calculated from different input models; the ability to reconstruct an input model from the synthetic data is then used to assess how well real structure can be constrained by the available data. We have used different synthetic input models, with harmonic wave speed variations as well as spike tests (for a discussion of such resolution tests, see, e.g., Humphreys and Clayton, 1988 or Spakman and Nolet, 1988), and others in which we tested the robustness of a specific structure in the model. Based on these tests and on theoretical considerations (Kennett and Nolet, 1990; Zielhuis, 1992; Zielhuis and van der Hilst,

1996) we conclude that the horizontal resolution in the best resolved parts of the continent approaches 250 km, and the vertical resolution ranges from 50 km (at 100 km depth) to between 100 and 150 km (around 300 km depth). As expected from the data coverage (Fig. 6), the resolution in the central and east is still superior to that in western Australia.

For the purpose of this paper we evaluated whether the data can constrain the wave speed variations on the length scales considered in the finest regionalization described below (see Section 5.4). In the experiment, different wave speeds were assigned to various tectonic regions of the Australian continent. Fig. 7 displays the results of two such tests. In the first, the

input anomalies of Fig. 7c were put at 80 km depth, with zero perturbations elsewhere in the model. We calculated synthetic data for all 1600 paths (both for fundamental modes and the overtones) and repeated the linearized inversion for 3D structure. The result for that layer is given in Fig. 7a. In the second experiment the input pattern (Fig. 7c) was placed at 210 km depth, with the response shown in Fig. 7b. These tests show that the wave speed variations are well resolved on the length scales we are interested in, but at shallow depth the image quality is better than at larger depth. In general wave speed contrasts are well resolved, but the amplitude of the wave speed variations is less well determined. We note

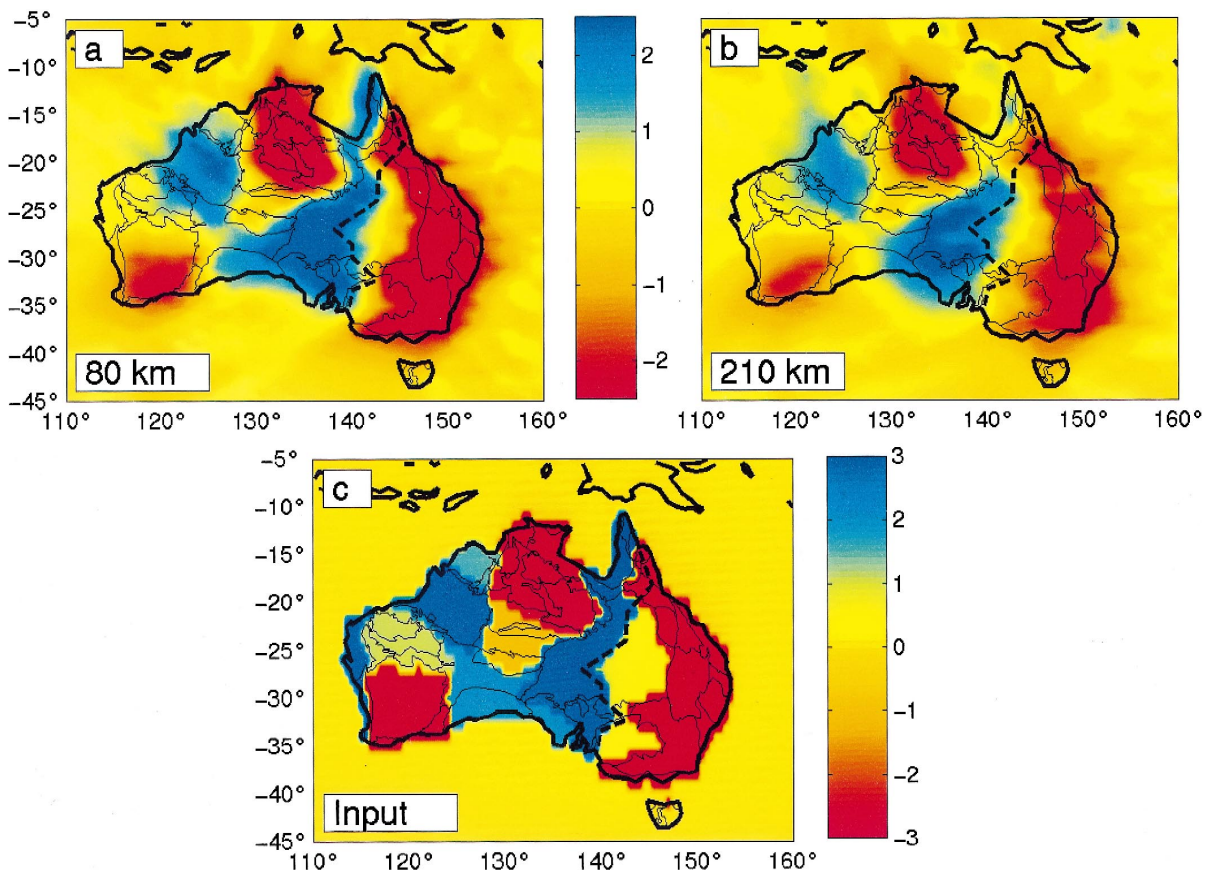


Fig. 7. Results of resolution experiment. Input models were constructed by assigning constant wave speed anomalies to different geotectonic regions and at different depths. Anomalies are in percent from a spherical reference model. Synthetic data were generated on the basis of all wave paths used in actual inversion. (a) Recovery of anomaly placed at 80 km. (b) Recovery at 210 km. (c) Input anomaly used in both tests. Note the difference between both color schemes. Thick dashed lines give approximate location of Tasman Line.

that in the regionalized presentation of our results (see Section 5.4) the wave speeds were averaged

over the regions identified, but in the test inversions shown here such averaging was not done.

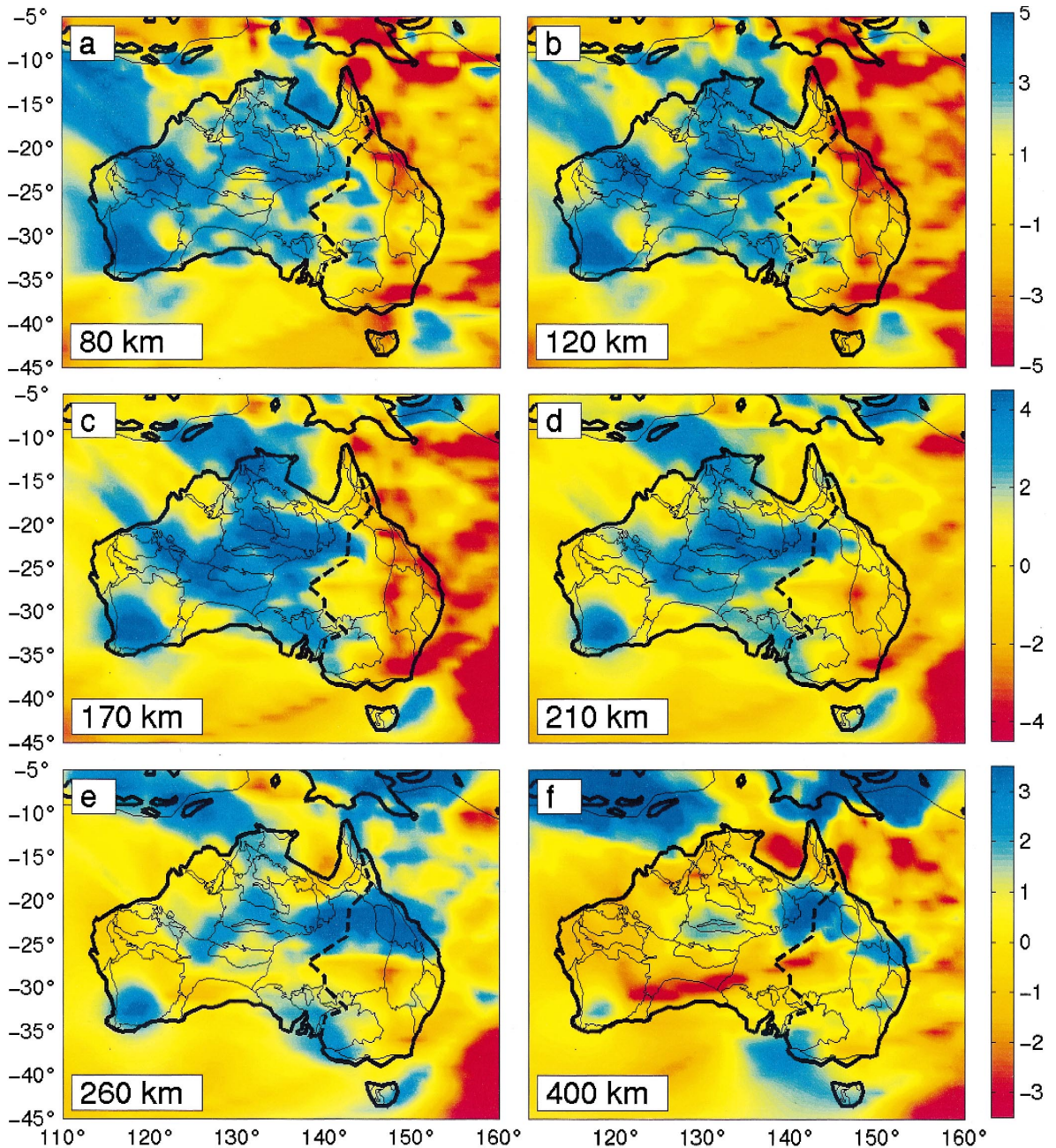


Fig. 8. Depth slices through our preferred velocity model. Anomalies are in percentage from a spherical reference model (see text). The reference velocities used are 4500 m s^{-1} at 80, 120, and 170 km depth (a–c); 4513.5 m s^{-1} at 210 km (d); 4581 m s^{-1} at 260 km (e), and 4851.5 m s^{-1} at 400 km depth (e). The color scales used are for a and b, c and d, and e and f, with diminishing values of saturation which reflects the decreasing magnitude of the anomalies with depth. Thick dashed lines give approximate location of Tasman Line.

5.2. Shear wave speed variations in the Australian upper mantle

Figs. 8 and 9 display some of the tomographic results. The shear wave speed anomalies ($\beta(r, \theta, \varphi) - \beta_0(r)$) are plotted as percentages of the wave speed in the reference model ($\beta_0(r)$) which is a modified version of PREM (without the discontinuity at 220 km). Wave propagation is slow beneath the Phanerozoic eastern part of Australia and fast beneath the Proterozoic and Archean domains, at least to a depth of 200 km (e.g., Fig. 8a–c and Fig. 9). The Phanerozoic high wave speed lithosphere is

relatively thin, generally less than 80 km (note the cross-sections have been cropped to show the depth range between 15 and 450 km), and overlies a pronounced low-velocity zone that extends to approximately 200 km depth (Fig. 9) (see also Goncz and Cleary, 1976; Goncz et al., 1975; and Zielhuis and van der Hilst, 1996).

In agreement with Zielhuis and van der Hilst (1996) our model reveals that at depths shallower than 150 km the wave speed gradient from the eastern to the central domains occurs east of where it would be expected on the basis of the exposure at the surface of Proterozoic rock (indicated by the

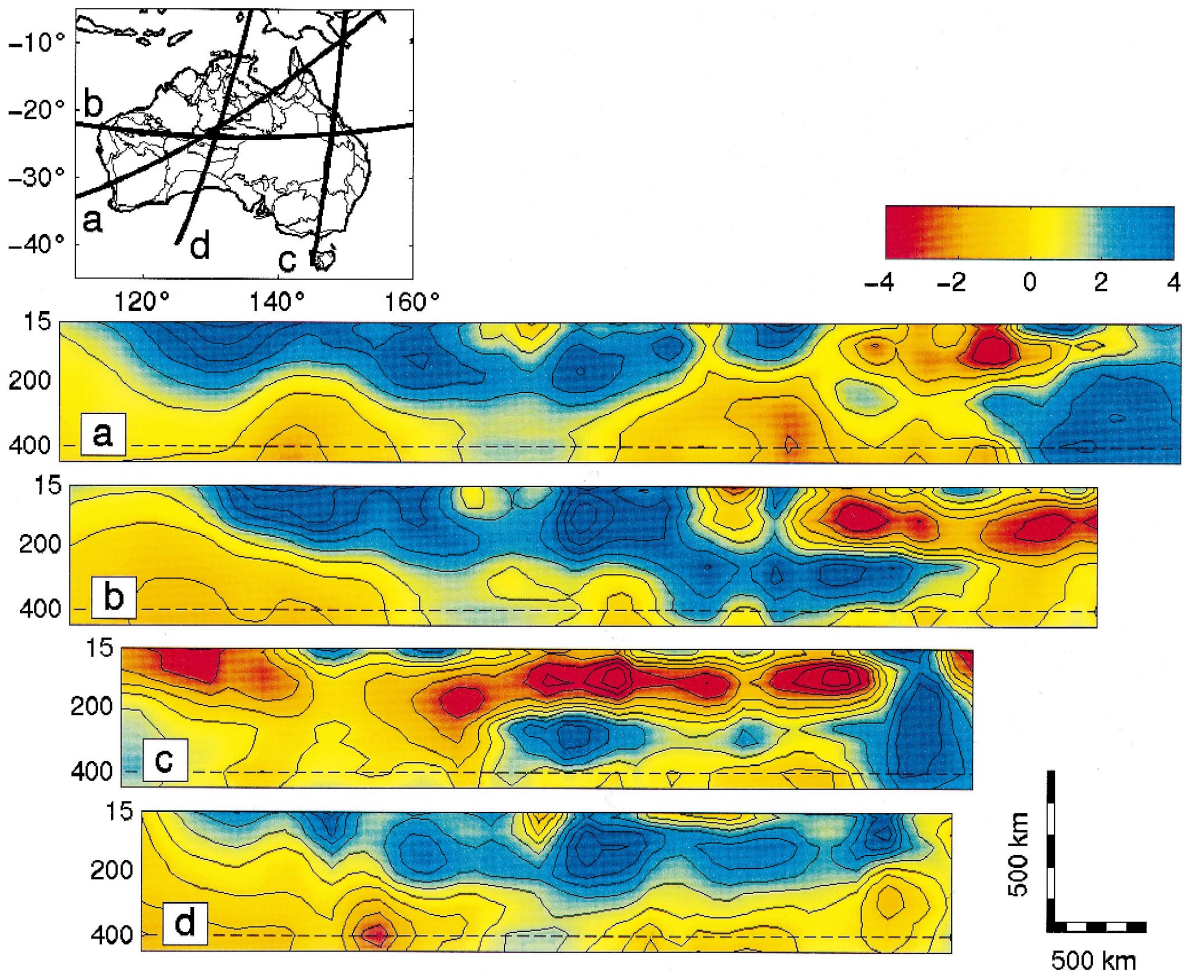


Fig. 9. Profiles through the model. Anomalies in percentage from a spherical reference model (see text). The high wave speeds in the northeastern corner of the map, which show at the right hand side of cross-sections (a) and (c), reflect the recent subduction of the Pacific beneath the Indo–Australian plate. The high wave speed feature to the southwest of Tasmania, (c), may be related to the Australia–Antarctic discordance (Gurnis et al., 1998) but this part of our model is not well sampled (see Fig. 6).

Tasman Line). The presence of high wave speed lithosphere east of the Tasman line was confirmed by the analysis of fundamental mode dispersion between stations along the same great-circle path (Passier et al., 1997) (Fig. 10). In several regions, the lateral wave speed contrast coincides with surface outlines of sedimentary basins in easternmost Australia, in particular the western margin of the Bowen and Surat basins. At greater depths the wave speed divide shifts westward, and at 170 and 210 km depth it appears to parallel the Tasman line and the western margin of the Eromanga basin. In northeastern Australia, the wave speed contrast is located to the west of the Georgetown Inlier, and this Proterozoic unit is

part of a rather thin high wave speed lid with a pronounced low velocity zone underneath (see Fig. 9). In contrast, the Proterozoic shields of central Australia are delineated by high wave speeds down to at least 250 km (e.g. between stations WRAB and SCOG in Fig. 10). The area of the Late-Paleozoic Alice Springs orogeny (Amadeus basin and Musgrave and Arunta blocks) stands out from the adjacent shields by lower wave speeds. This may reflect the thick layer of sediments in this region. Interestingly, also the Kimberley block, which is often interpreted as the westward continuation of the North Australia craton (see, e.g., Shaw et al., 1995 and Fig. 1b) has a seismic signature that differs significantly

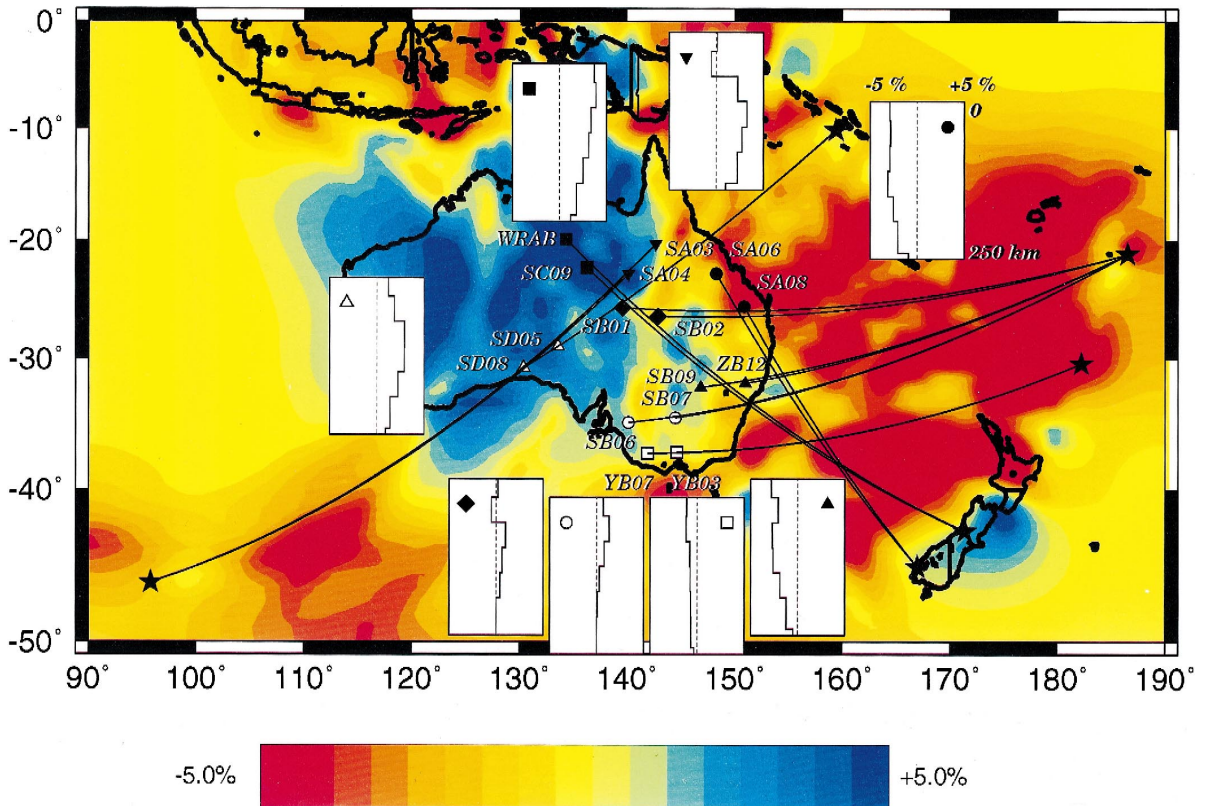


Fig. 10. Stations, events, great circle paths, and wave speed profiles at selected locations, superimposed on the shear wave speed variations at a depth of 140 km depth (Zielhuis and van der Hilst, 1996). The panels display wave speed variation to a depth of 250 km in eastern and central Australia as inferred from the differential dispersion of fundamental mode Rayleigh waves between stations along the same great circle path (Passier et al., 1997). In all velocity panels, perturbations range from -5% to 5% and the depth ranges from 0 to 250 km. (Modified after Passier et al., 1997). Note that our current models are based on more data than were available to Zielhuis and van der Hilst (1996).

from that of the Proterozoic craton. Likewise, the deep structure beneath the Canning basin differs from that beneath central Australia and from the Archean cratons further South (Fig. 8b–d).

Below 200 km depth the central cratons continue to be marked by fast anomalies, but the Archean Yilgarn, Pilbara, and Gawler cratons do not seem to be marked by wave speeds that are significantly higher than the reference model, with the exception of the localized high wave speeds under station

NWAO in the southern Yilgarn craton, but these might be an artifact of using one-dimensional sensitivity kernels (see Section 3.1). With the exception of the region encompassing the Alice Springs orogeny, the mantle beneath 300 km depth beneath the Proterozoic and Archean appears to be rather homogeneous. In this depth range, the most pronounced fast anomalies are associated with the subduction zones to the North and Northeast of Australia and with the intriguing structure east of the Mt.

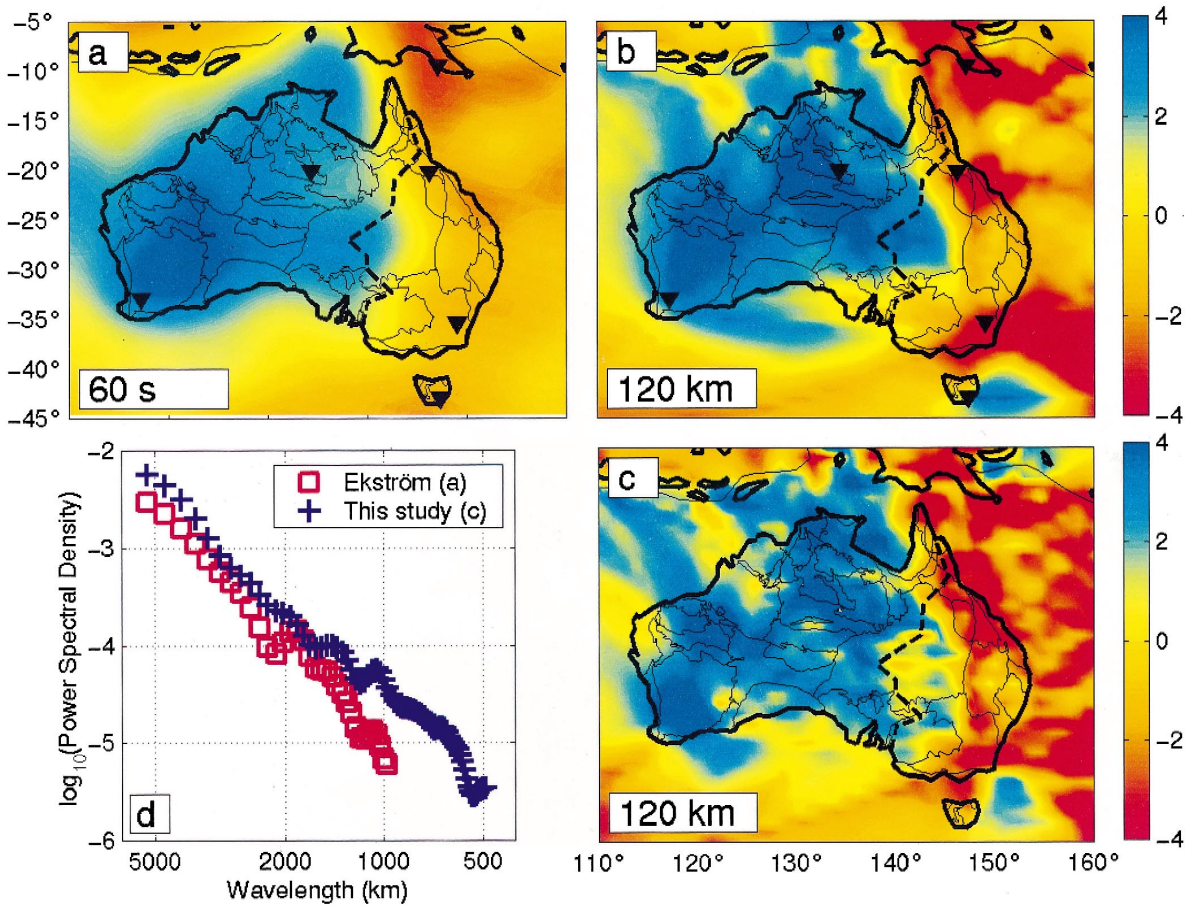


Fig. 11. Comparison with global model in spatial domain. Clockwise: (a) Rayleigh-wave inversion result by Ekström et al. (1997), at 60 s. This phase-velocity map records the anomalies of fundamental modes of some (narrow) frequency band around 60 s, or 17 mHz. From inspection of the kernels of Fig. 4, such map represents structural wave speed deviations with a maximum sensitivity around 120 km depth. We therefore compare it to our inversion results at those depths. (b) Wave speed anomalies at 120 km, using only fundamental modes from permanent seismometer stations (from IRIS and GEOSCOPE). The resolution of the result is roughly equivalent to the one in (a), with certain differences attributable to differences in path geometry. In (a) and (b), the location of the 6 permanent stations is indicated by the black triangles. (c) Our preferred model at 120 km depth. Thick dashed lines give approximate location of Tasman Line. (d) Power spectrum of the shear wave speed model at 80 km depth. The results are compared with the model by Ekström et al. (1997).

Isa block (at 23°S). Resolution tests and inversions with subsets of the data demonstrate that the latter anomaly is well resolved and required by the data used.

5.3. Global vs. regional models

Our regional model reveals variations in shear wave speed on smaller scales and with larger amplitude than indicated by global tomography models. To better understand such differences we compared our maps to the global images both in the spatial and spectral domains. Fig. 11a displays the wave speed variations according to the global model by Ekström et al. (1997), which contains information from about

1700, globally distributed earthquakes, and only a small number of permanent stations on or near the Australian continent. We obtain a similar result if we apply our inversion technique to fundamental mode data from the six regional IRIS and GEOSCOPE stations that were also used by Ekström et al. (1997) (Fig. 11b), although we retrieve somewhat lower wave speeds beneath the marginal basins east of Australia. Following Chevrot et al. (1998a,b) we also compared the power spectrum of our model with that from Ekström, which was parameterized in spherical harmonics up to degree 40, corresponding to a wavelength of about 1000 km. Across the entire spectrum our regional model does have somewhat higher amplitudes than the global model by Ekström et al.

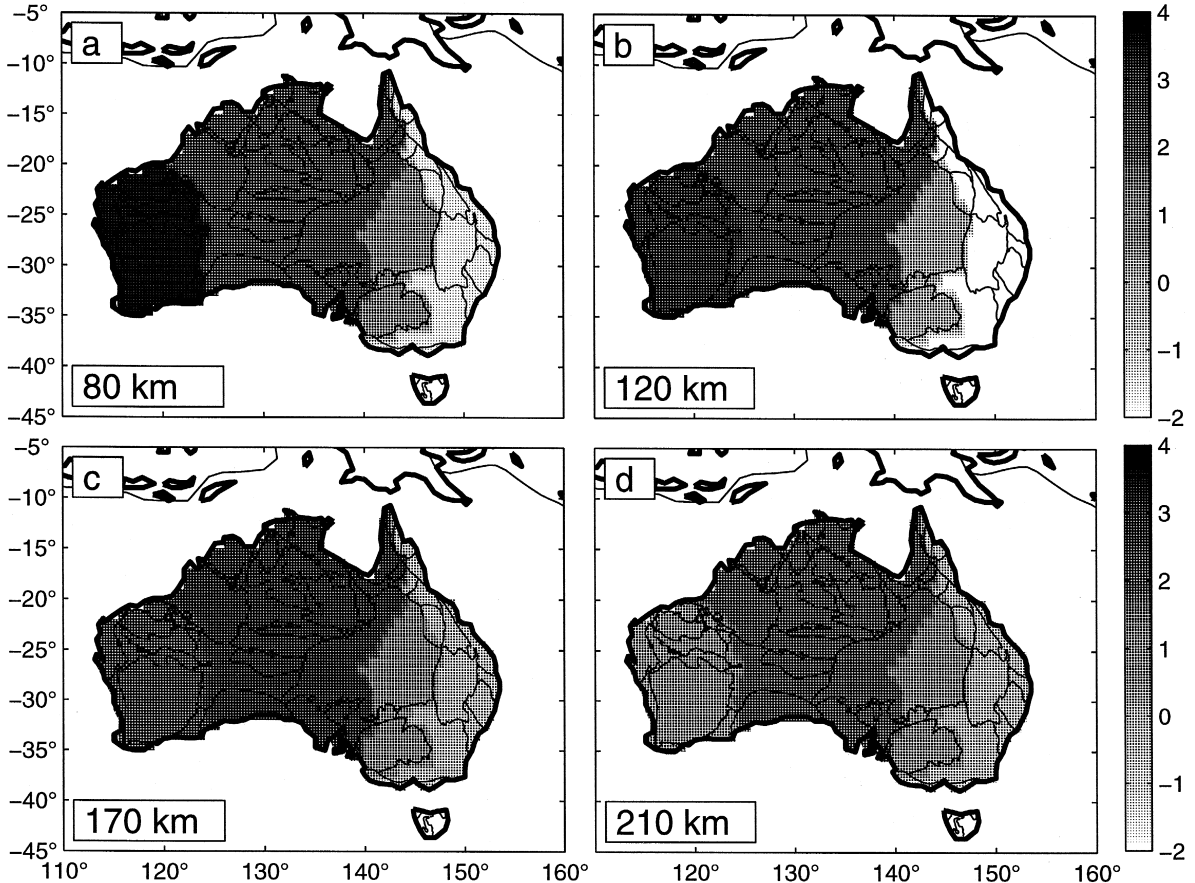


Fig. 12. Four-part regionalized representation of the shear wave speed model. This regionalization is based on large-scale variations in crustal age (see Fig. 1c).

(1997), but particularly so at wavelengths smaller than 2000 km (Fig. 11d). This is primarily a consequence of degrading resolution at those wavelengths in the global model (see Fig. 13 in Ekström et al., 1997). From this comparison we conclude that when evaluated at similar wavelengths the spatial and spectral characteristics of global and our regional models are generally in good agreement with each other, and the superior resolution at high wave numbers (comparing, e.g., Fig. 11a and c) is not dictated by the parameterization or damping but results from the dense data coverage provided by the Skippy

project and the inclusion of higher-mode Rayleigh waves.

5.4. Seismic signature of distinct tectonic regions

“Tectonic” regionalizations, whereby seismic properties are averaged over well-defined geological domains, have formed the basis of first-order testing of the tectosphere hypothesis (Jordan, 1975a, 1981b; Okal, 1977; Polet and Anderson, 1995), the synthesis of global seismic data (Nolet et al., 1994), and the calculation of travel-time corrections (Gudmundsson

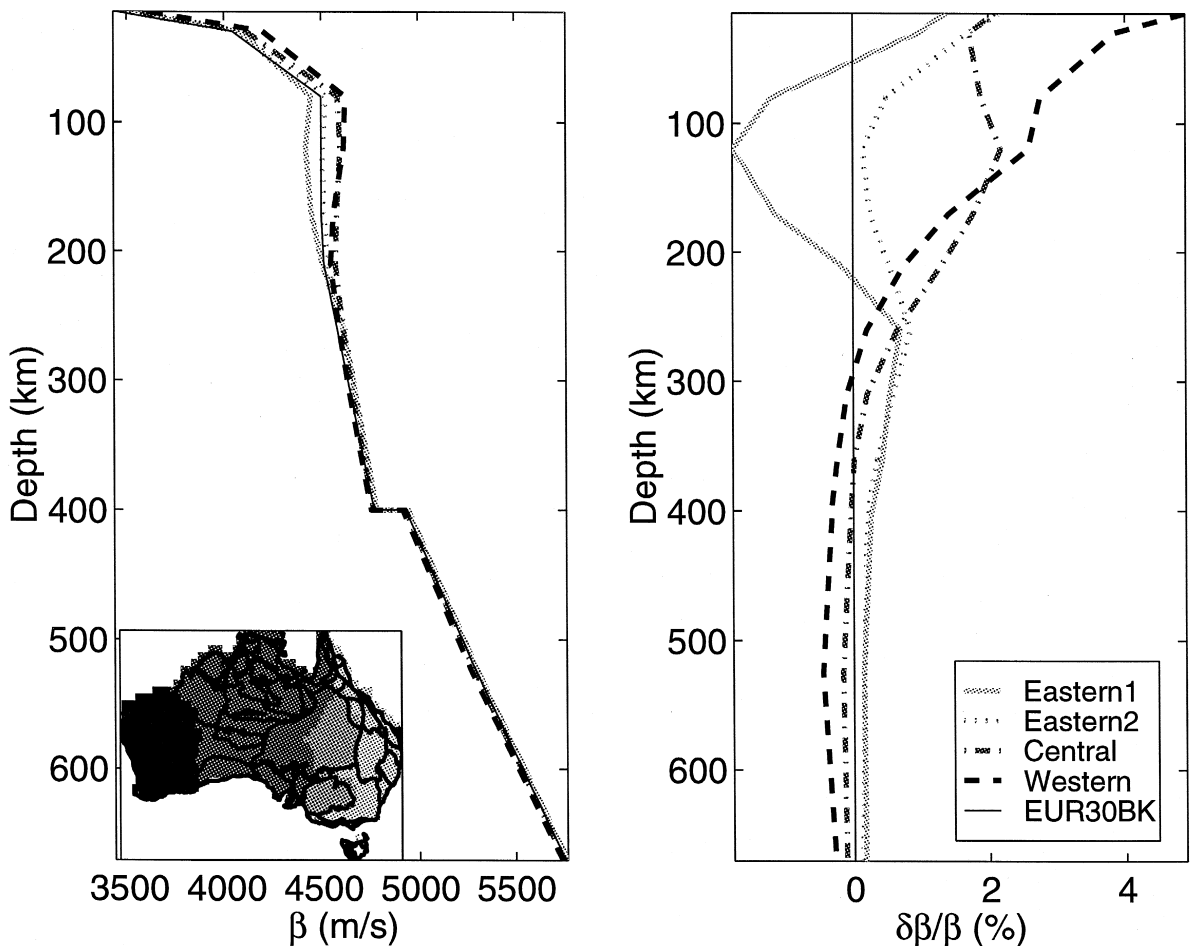


Fig. 13. Age-dependent wave speed variations with depth. (Left) Absolute wave speeds. (Right) Wave speed perturbations from a continental reference model. (Inset) Geographic location of the regions used (see Fig. 1c). Compare with Fig. 12 for a planview. Below ~ 250 km, the differences of average wave speed between those regions are an order of magnitude smaller than in the shallow mantle.

and Sambridge, 1998). We have used regionalizations to investigate the relationship between the

thickness of the high velocity lid and crustal age at different length scales.

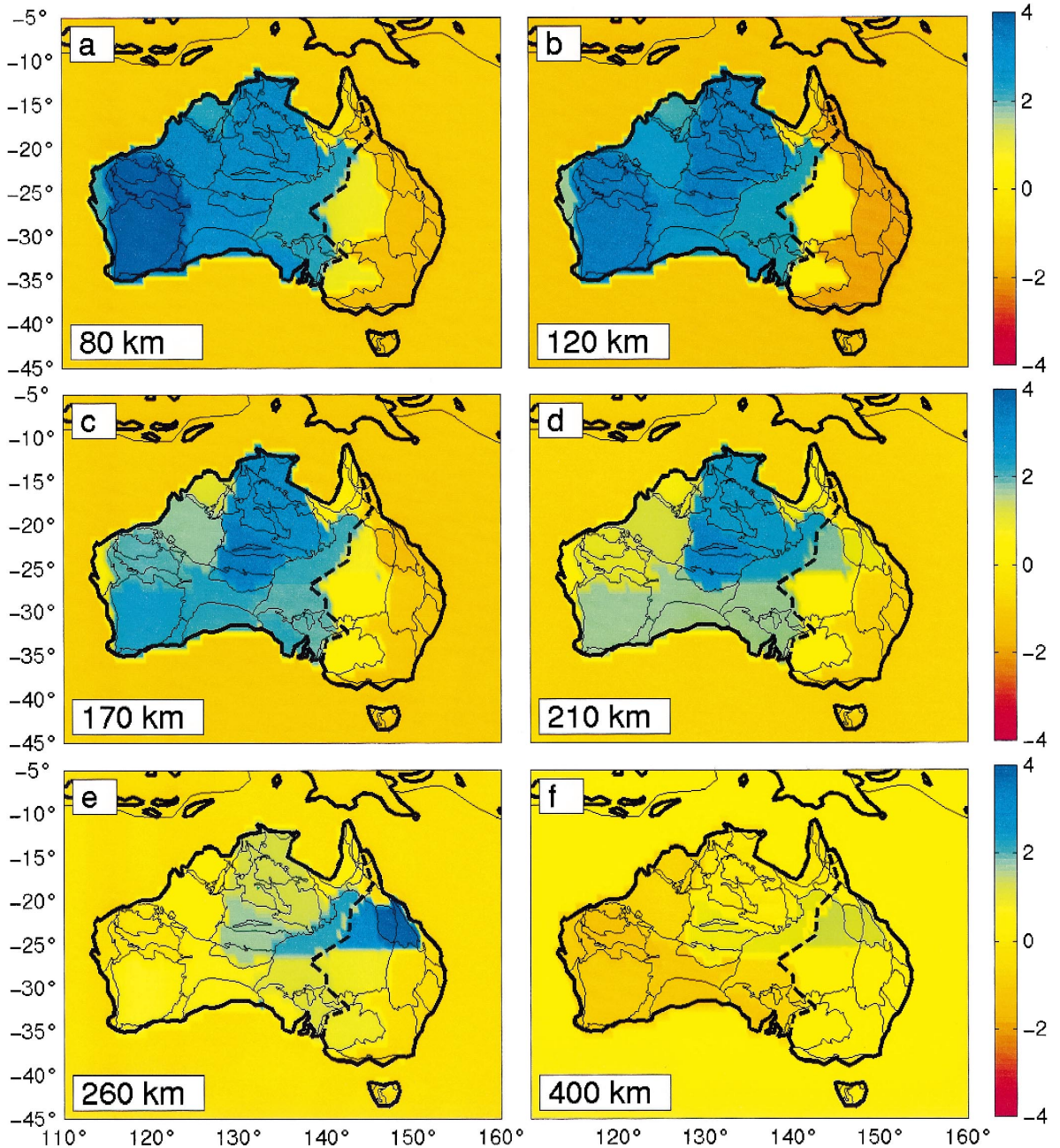


Fig. 14. Detailed regionalized representation of the shear wave speed model. In (a) and (c), a 12-part subdivision was chosen, whereas in (c–f), the domain centered over the Eromanga basin was subdivided to bring out the anomalous character of the fast structure centered at 23°S. For more discussion, see text. Thick dashed lines give approximate location of Tasman Line.

In our first experiment we used a three-fold tectonic regionalization based roughly on crustal age (Fig. 1c), with a further subdivision of the eastern domain in two parts motivated by wave speed maps (see Zielhuis and van der Hilst (1996) and Fig. 8). We averaged the wave speed perturbations over these domains. Fig. 12a–b shows the rather dramatic westward progression of seismic wave speed, which correlates well with the general increase in crustal age (Fig. 1c). However, deeper in the upper mantle this relationship breaks down and beneath 200 km depth the central Proterozoic is characterized by fast wave propagation while the average wave speeds in the Archean units are comparable to those under the Phanerozoic at large (Fig. 12c,d). Radial wave speed profiles, calculated for each domain, further illustrate that the recently tectonized eastern seaboard of Australia is generally slow, with a pronounced low-velocity zone centered around 150 km (Fig. 13). The Precambrian central and western parts do not show this reduction in wave speed; instead, the high-velocity lithosphere beneath these provinces is generally 200–250 km thick. Note that the Archean is faster than the Proterozoic for $z < 150$ km but that the high wave speed signature does not extend to as large a depth (Fig. 13). Our results are in general agreement with the results by Gaherty and Jordan (1996) and Gaherty et al. (1996) who argued for a difference of similar magnitude between fast continental and slow oceanic mantle to a depth exceeding 250 km.

It is obvious from geological maps and results of tomography that significant variations in crustal structure and seismic properties (and our ability to constrain them) occur on much smaller length scales than represented by the large scale regions discussed above. Therefore, we designed another regionalization based on geological units that better represent variations in tectonic age. This tectonic subdivision (Fig. 14) is based on the crustal elements map by Shaw et al. (1995) and refinements by Wellman (1998); it consists of a northern, central, western, and southern Australian domain, as well as the Tasman group and the New England fold belt (see Fig. 1b), and the Pinjarra (the southwestern-most part). On the basis of our wave speed maps (Fig. 8) we treat the Kimberley block separately from the northern Australian domain, the Canning basin apart from Central Australia, and the Pilbara apart from the

Yilgarn craton. In Fig. 14a,b we maintain our earlier division of the Tasman domain into a unit comprising the (western parts of the) Eromanga and Murray basins and a unit with the eastern Lachland and New England fold belts (see Fig. 1a). In Fig. 14c–f we have subdivided the Eastern and Western Tasman domain in a northern and southern part so as to prevent the anomalous fast structure centered around (145°E, 23°S) from biasing a larger region.

This regionalization (Fig. 14) largely confirms the westward progression of seismic signature at depths less than 200 km but also reveals significant departures of the general trends. The high wave speed in the Archean western Australian domain can largely be attributed to the Yilgarn block; the Pilbara block is not marked by higher-than-average wave speeds but resolution in this particular area may be lacking. Recall that the high wave speeds beneath the station NWA0 may be an artifact of using 1D kernels, and the signature of the Yilgarn region may thus be biased. The high wave speed under central Australia is mostly associated with the central block-and-basin structure and the North Australia craton. Beneath the Kimberley block and the Canning basin the pronounced positive wave speed anomalies vanish beneath 150 km depth, and at a slightly larger depth also the Archean Yilgarn, Pilbara, and Gawler units lose their deep seismic expression. However, the Proterozoic North Australia craton is still faster than average at depths in excess of 250 km. Surprisingly, the wave speed anomaly beneath the region encompassed by the Alice Springs orogeny seems to persist to depths in excess of 300 km. The upper mantle and transition zone beneath Eastern Australia seems more complex than its Precambrian counterpart (see also Fig. 9c and Section 5.2) and on average the transition beneath geological domains in eastern Australia are faster than in the west (Fig. 9b,c).

6. Discussion

The tectosphere concept as formulated by Jordan (1988) implies that the negative thermal buoyancy of the CLM is largely offset by changes in composition. Here we do not image composition and, therefore, use a less restricted definition. High wave speed lids that are more than ~ 200 km thick would be dynam-

ically unstable if the negative buoyancy owing to the low temperature is not somehow compensated by changes in composition (Jordan, 1975a,b; Anderson and Bass, 1984; Polet and Anderson, 1995; De Smet et al., 1999, this volume; Shapiro et al., 1999a,b, this volume). In the following we loosely refer to “continental keels” or “tectosphere” when the thickness of the high wave speed lid as inferred from our results exceeds this value.

6.1. Regional deviations from a global pattern

On the basis of global wave speed models, Jordan (1981b), Nolet et al. (1994), Polet and Anderson (1995), and others, concluded that there is a good agreement between the velocity anomalies and the surface pattern of crustal formation ages. The Precambrian domains are fast, whereas most Phanerozoic regions are underlain by a seismically slow upper mantle. Such observations have often been used to corroborate the correlation between crustal age and the composition of the CLM inferred from geological data. Global wave speed models have suggested that the high wave speeds persist down to 500 km depth (Su et al., 1994; Masters et al., 1996) but the depth extent of the high-velocity anomalies under stable continental regions has not been well constrained.

The fundamental and higher mode data used in our study are not consistent with these earlier results and, instead, constrain the thickness of the high wave speed CLM to less than 250–300 km. For Australia a strong correlation between surface age and seismic structure does exist, but only at long wavelengths ($\lambda > 1500$ km) and for depths shallower than ~ 200 km. At smaller length scales there are parts of Precambrian shields that are marked by high wave speeds to even larger depth but there are also many such regions without a deep seismic expression. At the length scales considered in our study, the “tectosphere” beneath the Proterozoic domains is as thick as or thicker than beneath Archean units, but the wave speed in the latter appears to be higher (Fig. 13). However, some Proterozoic domains, for instance the Georgetown Inlier in northern Queensland, are not marked by a deep, seismologically fast keel. On the other hand, some regions devoid of Proterozoic or older outcrop appear to have a tecto-

sphere-like CLM. Significant variations in seismic properties thus occur beneath geological provinces of comparable crustal age or tectonic setting and similar complexity may exist for other continents as well. Hence, for Australia there does not seem to be a simple relationship between tectosphere structure and crustal age.

6.2. Eastern Australia

Beneath easternmost Australia the high wave speed lid is thinner than 80 km in most places, entirely absent in some (for instance beneath the Queensland Volcanic Province), and mostly underlain by a pronounced low velocity zone centered at about 150 km depth (see Zielhuis and van der Hilst (1996) and references therein) (see also Figs. 9 and 13). Tectonically this area is relatively young, and in the southeast volcanism may have ceased only a few thousand years ago (Johnson, 1989). The geothermal gradient is steep, the present-day surface heat-flow is high (70–100 mW m⁻²) (Cull and Denham, 1979), and studies of mantle conductivity (Lilley et al., 1981; Finlayson, 1982) suggest that volatile-rich material or partial melt may be present. Therefore, the pervasive lower-than-average wave speeds in this region are most likely the result of thermal processes associated with the Late-Cretaceous (~ 80 Ma) opening of the Tasman Sea and accompanying volcanism (Storey, 1995), volatile infusion during subduction prior to that event, and the recent volcanism in the region.

To the west of the low wave speed region, but still east of the Tasman line, the wave speed signature suggests the presence of a seismically fast root. Although it is not as thick as the CLM beneath the Proterozoic proper, this could imply that some of the early Paleozoic fold belts (for example the Adelaidean and western part of the Lachland) and basins (e.g., western part of the Murray basin) are underlain by Precambrian basement (Zielhuis and van der Hilst, 1996). This interpretation, which was recently corroborated by Re-Os model ages of up to 1.96 Ga for upper mantle xenoliths in western Victoria (Handler et al., 1997), would have implications not only for understanding the structural development of these fold belts and basins but also for the paleogeographic reconstruction of the Rodinia supercontinent (Powell, 1998; K. Karlstrom, pers. comm., 1999).

It is unlikely that the anomalously fast structure at a depth greater than 250 km, i.e., beneath the pronounced low velocity zone (see Fig. 8c–fFig. 9b), is related to stable lithospheric structure formed *in situ*. Instead it may represent allochthonous material. Perhaps it represents one or more accreted terranes of continental tectosphere that was originally formed elsewhere. Given the north-northeastward motion of the Australian plate relative to the lower mantle (DeMets et al., 1990), a perhaps more plausible explanation is that fragments of formerly oceanic lithosphere that were subducted beneath the island arcs to the north and northeast of Australia have subsequently been overridden by the continent.

6.3. Central and Western Australia

As mentioned above, the seismic signature of the tectosphere in central and western Australia changes significantly within geological provinces of comparable age and tectonic setting, and the thickest tectosphere appears to be associated with the Proterozoic shields, not with the Archean cratons. Moreover, some of the fast anomalies beneath central and eastern Australia do not correlate with surface geology in an obvious fashion. A detailed interpretation of these observations is beyond the scope of this paper, but we speculate on a few scenarios that might explain the observed complexity.

Assuming that the interpretation of the thick high wave speed structure in terms of stable continental keels (tectosphere) is basically correct, two fundamentally different explanations can be given. One possibility is that the differences within and between the Archean–Proterozoic provinces are entirely due to how the structures were originally formed, and have persisted ever since. Conditions for melt depletion associated with tectosphere formation could have varied from region to region. However, this complexity is not readily consistent with the correlation between crustal age and mantle composition inferred from geological data (e.g., Griffin et al. (1998)), which implies a certain uniformity of formation processes. Another explanation is that a thick ($z > 250$ km) tectosphere formed everywhere but only survived beneath central Australia. Shapiro et al. (1999a) showed that a cold tectosphere could be supported by high viscosity alone but that compositional buoy-

ancy is required to annihilate part of the gravity signal and to stabilize the “keel” during formation when the temperature was higher and the viscosity lower. The CLM can be eroded by later thermal processes, which would reduce its viscosity, in particular when it is already weakened by hydration, for example by volatile infusion during subduction (Nolet and Zielhuis, 1994). The removal of CLM by plumes, subduction, or small-scale convection associated with continental break-up has been invoked to explain the deep structure beneath western part of the Russian Platform (Nolet and Zielhuis, 1994), the anomalously low subcrustal P_n and S_n velocities beneath the southwestern margin of the Proterozoic Baltic Shield (Bannister et al., 1991), and the absence of a seismically fast CLM beneath the Rocky Mountain front in North America (Egglar et al., 1988), the Proterozoic Grenville province in the eastern part of United States (van der Lee and Nolet, 1997b), and the Archean Sino–Korean craton (see Griffin et al., 1998 and references therein). The position of the “rootless” Archean Yilgarn, Pilbara, and Gawler blocks near passive margins suggests that an original deep high-velocity lid could have been destroyed by convective processes associated with continental break-up when western and southern Australia parted from India and Gondwana (onset ~ 130 Ma) and Antarctica (starting ~ 80 Ma) (Veevers, 1984). Much like the rifting of Australia from New Zealand, the separation of Greater India from Australia was preceded and accompanied by extensive magmatism and related thermal processes (Storey, 1995).

Alternatively, the deep ($z > 200$ km) high wave speeds represent temperature perturbations associated with subcontinental downwellings instead of stable tectosphere. This may apply to the localized high wave speed structure beneath the central Australian region involved in the Late-Paleozoic Alice Springs orogeny, which may continue to lower mantle depths (Grand, 1998, pers. comm.). In this scenario, the permanent thick part of the continental plate might have an almost uniform thickness of about 200–250 km beneath all domains of Archean or Proterozoic age, and the deep, high-velocity anomalies under central and northern Australia reflect convective instabilities under the continent. Cold convective drips beneath continents have been sug-

gested before (Gurnis, 1988; De Smet et al., 1999, this volume) and were invoked to explain the deep high wave speeds beneath the Canadian shield (Pari and Peltier, 1996) (see, however, Shapiro et al., 1999b). For North America, Li et al. (1998) showed that the undulations of the 410 km discontinuity, which marks the isochemical phase change from olivine to wadsleyite, are small and do not correlate with the presence of a cold CLM. From this they conclude that the cold drips must be small, if they exist at all. For Australia such studies have not yet been completed.

7. Conclusions

We have analyzed about 1600 broad-band, vertical-component seismograms provided by the permanent IRIS, GEOSCOPE, and AGSO stations and the portable seismograph stations of the SKIPPY project. The combination of dense wave-path coverage and the use of both the fundamental and higher modes of the Rayleigh (surface) wave allowed us to delineate aspherical wave speed variations of the Australian continent in unprecedented detail. Our current inversions account for isotropic wave speed variations only. In this paper we have focused on the presentation of the results, with special emphasis on the relation between wave speed variations in the upper mantle and the geological age of the overlying crust. In order to investigate whether that relationship depends on length scale of the wave speed variations and crustal structures considered, we have performed different tectonic regionalizations of our new wave speed model. We reach the following conclusions:

(1) For large scale lengths, and above ~ 200 km, there is a dramatic westward progression of lithospheric wave speed with increasing crustal age, in agreement with global studies. In general, the Phanerozoic lithosphere (< 80 km thick) is underlain by low velocity anomalies (with respect to a continental reference model); such a LVZ is absent beneath the Precambrian units, which instead are underlain by fast *S*-wave anomalies to about 200–300 km depth.

(2) Even on these large scales ($\lambda > 1500$ km) the high wave speed lid of the Proterozoic provinces (central Australia) is generally thicker (250–300 km)

than that of the Archean cratons (175–250 km), but the wave speed anomalies are higher in the latter. Our estimates of the thickness of the Archean CLM are slightly larger than, but given the uncertainty, consistent with, those of the Kaapvaal craton (Priestley, 1999, this volume).

(3) The Early-Paleozoic mountain belts in southeastern Australia (Adelaidean and western Lachland) and the western part of the Phanerozoic Murray basin are underlain by tectosphere-like upper mantle (~ 150 km thick). The inference that crustal deformation has occurred on a Proterozoic ramp is consistent with mid-Proterozoic Re-Os ages for upper mantle xenoliths from the Mt. Gambier volcanic complex several hundred km east of the outcrop divide (the so-called Tasman line) between the Proterozoic central shields and the Phanerozoic fold belts (Handler et al., 1997). These observations are important for understanding the extent of Precambrian lithosphere in Australia as well as the reconstruction of the Proterozoic super-continent Rodinia.

(4) The high wave speed structures that we interpret as old continental keels often continue off-shore, for instance northward into New Guinea, and southward into the Indian Ocean. The latter may represent stretched continental lithosphere resulting from rifting between Australia and Antarctica. Likewise, the inferred high wave speed keel just east of the Tasman Line could represent thinned lithosphere due to extension associated with the break-up of Rodinia (post-750 Ma).

(5) At shorter wavelengths, parts of the Precambrian shields are underlain by high wave speeds to depths greater than 200 km but other such domains lack a deep seismic signature altogether.

(6) The large variability of the seismic signature of the deep continent may be explained by (1) as yet poorly understood differences in the original fractionation and depletion of the upper mantle and — more likely — (2) the local disruption and removal of once thick tectosphere by later tectonic processes. We notice that the ‘‘rootless’’ Archean cratons are located near old passive plate margins, suggesting that destabilization of tectospheric mantle has occurred by small-scale convection associated with continental break-up and subsequent rifting. Alternatively, some of the deep high wave speed structures may reflect cold downwellings (e.g., beneath central

Australia) or the relics of allochthonous terranes (either exotic tectospheric blocks accreted onto eastern Australia, or remnants of subducted slab overridden by the plate on its northeastwardly journey).

(7) Variations in deep continental structure within regions of similar crustal age and tectonic setting are significant and often as large as variations between such age units. This implies that the wave speed models do not always support a simple relationship between mantle composition and crustal age and that global correlations based on geological regionalizations on scales smaller than about 1000 km should be considered with caution.

Acknowledgements

We are grateful to Brian Kennett at the Australian National University for his support of the SKIPPY project and for many discussions about the structure of the Australian continent. We thank Mark Leonard at the Australian Geological Survey Organisation for help in making the AGSO-data available to us. We thank Erik Larson, Roberta Rudnick, and Bill McDonough for thoughtful comments on the manuscript, and Bill McDonough for expediting the review process. This research was supported by the National Science Foundation, grant EAR-9614341.

References

- Aki, K., Richards, P.G., 1980. *Quantitative Seismology*. Freeman, San Francisco, CA.
- Anderson, D.L., Bass, J.D., 1984. Mineralogy and composition of the upper mantle. *Geophys. Res. Lett.* 11, 637–640.
- Bannister, S.C., Ruud, B., Husebye, E.S., 1991. Tomographic estimates of sub-Moho seismic velocities in Fennoscandia and structural implications. *Tectonophysics* 189, 37–53.
- Bostock, M., 1999. Seismic imaging of lithospheric discontinuities and continental evolution. In: van der Hilst, R.D., McDonough, W., (Eds.), *Composition, Deep Structure and Evolution of Continents*. Elsevier.
- Boyd, F.R., 1989. Compositional distinction between oceanic and cratonic lithosphere. *Earth Planet. Sci. Lett.* 96, 15–26.
- Boyd, F.R., Gurney, J.J., 1986. Diamonds and the African lithosphere. *Science* 232, 472–477.
- Burke, K., Kind, W., 1978. Were Archean continental geothermal gradients much steeper than those of today?. *Nature* 272, 240–241.
- Cara, M., 1979. Lateral variations of *S*-velocity in the upper mantle from higher Rayleigh modes. *Geophys. J. R. Astron. Soc.* 5, 649–670.
- Chevrot, S., Montagner, J.-P., Snieder, R.K., 1998a. The spectrum of tomographic Earth models. *Geophys. J. Int.* 133, 783–788.
- Chevrot, S., Montagner, J.-P., Snieder, R.K., 1998b. The spectrum of tomographic Earth models: correction. *Geophys. J. Int.* 135, 311.
- Cichowicz, A., Green, R., 1992. Tomographic study of upper-mantle structure of the South-African continent, using waveform inversion. *Phys. Earth Planet. Inter.* 72, 276–285.
- Clitheroe, G., Gudmundsson, O., Kennett, B.L.N., submitted. The crustal structure of Australia. *J. Geophys. Res.*
- Cull, J.P., Denham, D., 1979. Regional variations in Australian heat flow. *BMR J. Aust. Geol. Geophys.* 4, 1–13.
- Dahlen, F.A., 1976. Models of the lateral heterogeneity of the Earth consistent with eigenfrequency splitting data. *Geophys. J. R. Astron. Soc.* 44, 77–105.
- Dahlen, F.A., Tromp, J., 1998. *Theoretical Global Seismology*. Princeton Univ. Press, Princeton, NJ.
- De Smet, J.H., van den Berg, A.P., Vlaar, N.J., 1999. The evolution of continental roots in numerical thermo-chemical mantle convection models including differentiation by partial melting. In: van der Hilst, R.D., McDonough, W. (Eds.), *Composition, Deep Structure and Evolution of Continents*. Elsevier.
- DeMets, C., Gordon, R.G., Angus, D.F., Stein, S., 1990. Current plate motions. *Geophys. J. Int.* 101, 425–478.
- Dziewonski, A.M., Anderson, D.L., 1981. Preliminary reference earth model. *Phys. Earth Planet. Inter.* 25, 297–356.
- Dziewonski, A.M., Chou, T.-A., Woodhouse, J.H., 1981. Determination of earthquake source parameter from waveform data for studies of global and regional seismicity. *J. Geophys. Res.* 86, 2825–2852.
- Eggler, D.H., Keen, J.K., Welt, F., Dudas, F.O., Furlong, K.P., McCallum, M.E., Carlson, R.W., 1988. Tectonomagmatism of the Wyoming Province. *Colorado School of Mines Quarterly* 83, 25–40.
- Ekström, G., Tromp, J., Larson, E.W.F., 1997. Measurements and global models of surface wave propagation. *J. Geophys. Res.* 102, 8137–8157.
- Engdahl, E., van der Hilst, R.D., Buland, R., 1998. Global teleseismic earthquake relocation with improved travel times and procedures for depth determination. *Bull. Seis. Soc. Am.* 88, 722–743.
- Finlayson, D.M., 1982. Geophysical differences in the lithosphere between Phanerozoic and Precambrian Australia. *Tectonophysics* 84, 287–312.
- Gaherty, J.B., Jordan, T.H., 1996. Lehmann discontinuity as the base of an anisotropic layer beneath continents. *Science* 268, 1468–1471.
- Gaherty, J.B., Jordan, T.H., Gee, L.S., 1996. Seismic structure of the upper mantle in a central Pacific corridor. *J. Geophys. Res.* 101, 22291–22309.
- Goncz, J., Cleary, J.R., 1976. Variations in the structure of the upper mantle beneath Australia, from Rayleigh wave observations. *Geophys. J. R. Astron. Soc.* 44, 507–516.
- Goncz, J.H., Hales, A.L., Muirhead, K.J., 1975. Analysis to

- extended periods of Rayleigh and Love wave dispersion across Australia. *Geophys. J. R. Astron. Soc.* 41, 81–108.
- Griffin, W.L., O'Reilly, S.Y., Ryan, C.G., Gaul, O., Ionov, D.A., 1998. Secular variation in the composition of subcontinental lithospheric mantle: Geophysical and geodynamic implications. In: Braun, J., Dooley, J., Goleby, B., van der Hilst, R.D., Klootwijk, C. (Eds.), *Structure and Evolution of the Australian Continent*. AGU Geodynamics Series, AGU, Washington, DC, pp. 1–26.
- Gudmundsson, O., Sambridge, M., 1998. A regionalized upper mantle (RUM) seismic model. *J. Geophys. Res.* 103, 7121–7136.
- Gurnis, M., 1988. Large-scale mantle convection and the aggregation and dispersal of supercontinents. *Nature* 332, 695–699.
- Gurnis, M., Müller, R.D., Moresi, L., 1998. Cretaceous vertical motion of Australia and the Australian–Antarctic discordance. *Science* 279, 1499–1504.
- Handler, M.R., Bennett, V., Esat, T., 1997. The persistence of off-cratonic lithospheric mantle: Os isotopic systematics of variably metasomatised southeast Australian xenoliths. *Earth Planet. Sci. Lett.* 151, 61–75.
- Herman, G.T. (Ed.), 1979. *Image reconstruction from projections*, Vol. 32 of *Topics in Applied Physics*. Springer-Verlag, Berlin, Germany.
- Humphreys, E.D., Clayton, R., 1988. Adaptation of back projection tomography to seismic travel time problems. *J. Geophys. Res.* 93, 1073–1085.
- Jaupart, C., Mareschal, J.-C., 1999. Thermal structure and thickness of continental roots. In: van der Hilst, R.D., McDonough, W. (Eds.), *Composition, Deep Structure and Evolution of Continents*. Elsevier.
- Johnson, R.W. (Ed.), 1989. *Intraplate Volcanism in Eastern Australia and New Zealand*. Cambridge Univ. Press, Melbourne, Australia.
- Jordan, T.H., 1975a. Lateral heterogeneity and mantle dynamics. *Nature* 257, 745–750.
- Jordan, T.H., 1975b. The continental tectosphere. *Rev. Geophys.* 13, 1–12.
- Jordan, T.H., 1978. Composition and development of the continental tectosphere. *Nature* 274, 544–548.
- Jordan, T.H., 1981a. Continents as a chemical boundary layer. *Phil. Trans. Roy. Soc. Lond., Series A* 301, 359–373.
- Jordan, T.H., 1981b. Global tectonic regionalization for seismological data analysis. *Bull. Seism. Soc. Am.* 71, 1131–1141.
- Jordan, T.H., 1988. Structure and formation of the continental tectosphere. *J. Petrol., Special Lithosphere Issue*, 11–37.
- Kaula, W.M., 1967. Geophysical applications of satellite determinations of the Earth's gravitational field. *Space Sci. Rev.* 7, 769–794.
- Kennett, B.L.N., 1984. Guided wave propagation in laterally varying media — I. Theoretical development. *Geophys. J. R. Astron. Soc.* 79, 235–255.
- Kennett, B.L.N., 1995. Approximations for surface-wave propagation in laterally varying media. *Geophys. J. Int.* 122, 470–478.
- Kennett, B.L.N., Nolet, G., 1990. The interaction of the *S*-wave field with upper mantle heterogeneity. *Geophys. J. Int.* 101, 751–762.
- Kennett, B.L.N., Engdahl, E., Buland, R., 1995. Constraints on seismic velocities in the Earth from travel-times. *Geophys. J. Int.* 122, 108–124.
- Lambeck, K., 1983. Structure and evolution of the intracratonic basins of central Australia. *Geophys. J. R. Astron. Soc.* 74, 843–886.
- Laske, G., Masters, G., 1996. Constraints on global phase velocity maps from long-period polarization data. *J. Geophys. Res.* 101, 16059–16075.
- Lay, T., Wallace, T.C., 1995. *Modern Global Seismology*. Academic Press, San Diego, CA.
- Lenardic, A., 1998. On the partitioning of mantle heat loss below oceans and continents over time and its relationship to the Archaean paradox. *Geophys. J. Int.* 134, 706–720.
- Li, A., Fischer, K.M., Wyssession, M.E., Clarke, T.J., 1998. Mantle discontinuities and temperature under the North American continental keel. *Nature* 395, 160–163.
- Li, X.-d., Tanimoto, T., 1993. Waveforms of long-period body waves in a slightly aspherical Earth model. *Geophys. J. Int.* 112, 92–102.
- Lilley, F.E.M., Woods, D.V., Sloane, M.N., 1981. Electrical conductivity from Australian magnetometer arrays using spatial gradient data. *Phys. Earth Planet. Inter.* 25, 202–209.
- Marquering, H., Snieder, R., 1995. Surface-wave mode coupling for efficient forward modelling and inversion of body-wave phases. *Geophys. J. Int.* 120, 186–208.
- Marquering, H., Snieder, R., 1996. Shear-wave velocity structure beneath Europe, the Northeastern Atlantic and Western Asia from waveform inversions including surface-wave mode coupling. *Geophys. J. Int.* 127, 283–304.
- Marquering, H., Snieder, R., Nolet, G., 1996. Waveform inversions and the significance of surface-wave mode coupling. *Geophys. J. Int.* 124, 258–278.
- Masters, G., Johnson, S., Laske, G., Bolton, H., 1996. A shear-velocity model of the mantle. *Phil. Trans. R. Soc. Lond., Series A* 354, 1385–1410.
- Menke, W., 1989. *Geophysical Data Analysis: Discrete Inverse Theory*, Vol. 45 of *International Geophysics Series*, 2nd edn., Academic Press, San Diego.
- Murray, C.G., Scheibner, E., Walker, R.N., 1989. Regional geological interpretation of a digital coloured residual Bouguer gravity image of eastern Australia with a wavelength cut-off of 250 km. *Aust. J. Earth Sci.* 36, 423–449.
- Nolet, G., 1985. Solving or resolving inadequate and noisy tomographic systems. *J. Comput. Phys.* 61, 463–482.
- Nolet, G. (Ed.), 1987. *Seismic Tomography*. Reidel, Dordrecht, The Netherlands.
- Nolet, G., 1990. Partitioned waveform inversion and two-dimensional structure under the network of autonomously recording seismographs. *J. Geophys. Res.* 95, 8499–8512.
- Nolet, G., Zielhuis, A., 1994. Low *S*-velocities under the Tornquist–Teisseyre zone — Evidence for water injection into the transition zone by subduction. *J. Geophys. Res.* 99, 15813–15820.
- Nolet, G., van Trier, J., Huisman, R., 1986. A formalism for nonlinear inversion of seismic surface waves. *Geophys. Res. Lett.* 13, 26–29.

- Nolet, G., Grand, S.P., Kennett, B.L.N., 1994. Seismic heterogeneity in the upper mantle. *J. Geophys. Res.* 99, 23753–23766.
- Nyblade, A.A., 1999. Heat flow and the structure of Precambrian lithosphere. In: van der Hilst, R.D., McDonough, W. (Eds.), *Composition, Deep Structure and Evolution of Continents*. Elsevier.
- Okal, E.A., 1977. The effect of intrinsic oceanic upper-mantle heterogeneity on regionalization of long-period Rayleigh-wave phase velocities. *Geophys. J. R. Astron. Soc.* 49, 357–370.
- Paige, C.C., Saunders, M.A., 1982. LSQR: An algorithm for sparse linear equations and sparse least squares. *ACM Trans. Math. Software* 8, 43–71.
- Pari, G., Peltier, W.R., 1996. The free-air gravity constraint on subcontinental mantle dynamics. *J. Geophys. Res.* 101, 28105–28132.
- Passier, M., van der Hilst, R.D., Snieder, R.K., 1997. Surface wave waveform inversions for local shear-wave velocities under eastern Australia. *Geophys. Res. Lett.* 24, 1291–1294.
- Pearson, D., 1999. The age of continental roots. In: van der Hilst, R.D., McDonough, W. (Eds.), *Composition, Deep Structure and Evolution of Continents*. Elsevier, 1999.
- Pearson, D.G., Snyder, G., Shirey, S., Taylor, L., Carlson, R.W., Sobolev, N., 1995. Archean Re-Os age for Siberian eclogites and constraints on Archean tectonics. *Nature* 374, 711–713.
- Plumb, K.A., 1979. The tectonic evolution of Australia. *Earth Sci. Rev.* 14, 205–249.
- Polet, J., Anderson, D.L., 1995. Depth extent of cratons as inferred from tomographic studies. *Geology* 23, 205–208.
- Powell, C., 1998. Break-up of Rodinia in Australia; Implications for the western margin of Laurentia. In: *Abstracts with Programs, Geological Society of America, 1998 Annual Meeting, Vol. 30*. Geological Society of America, p. 47.
- Priestley, K., 1999. Velocity structure of the continental upper mantle: Evidence from South Africa. In: van der Hilst, R.D., McDonough, W. (Eds.), *Composition, Deep Structure and Evolution of Continents*. Elsevier.
- Richardson, S.H., Gurney, J., Erlank, A.J., Harris, J.W., 1984. Origin of diamonds in old enriched mantle. *Nature* 310, 198–202.
- Richter, F.M., 1984. Regionalized models for the thermal evolution of the Earth. *Earth Planet. Sci. Lett.* 68, 471–484.
- Richter, F.M., 1985. Models for the Archean thermal regime. *Earth Planet. Sci. Lett.* 73, 350–360.
- Richter, F.M., 1988. A major change in the thermal state of the Earth at the Archean–Proterozoic boundary: Consequences for the nature and preservation of continental lithosphere. *J. Petrol., Special Lithosphere Issue*, 39–52.
- Slater, J.G., Parsons, B., Jaupart, C., 1981. Oceans and continents: Similarities and differences in the mechanisms of heat loss. *J. Geophys. Res.* 86, 11535–11552.
- Shapiro, S.S., Hager, B.H., Jordan, T.H., 1999a. Stability and dynamics of the continental tectosphere. In: van der Hilst, R.D., McDonough, W. (Eds.), *Composition, Deep Structure and Evolution of Continents*. Elsevier.
- Shapiro, S.S., Hager, B.H., Jordan, T.H., 1999b. The continental tectosphere and Earth's long-wavelength gravity field. In: van der Hilst, R.D., McDonough, W. (Eds.), *Composition, Deep Structure and Evolution of Continents*. Elsevier.
- Shaw, R.D., Wellmann, P., Gunn, P., Whitaker, A.J., Tarlowski, C., Morse, M.P., 1995. Australian crustal elements map. *AGSO Res. Newslett.* 23, 1–3.
- Shibutani, T., Sambridge, M., Kennett, B.L.N., 1996. Genetic algorithm inversion for receiver functions with application to crust and uppermost mantle structure beneath eastern Australia. *Geophys. Res. Lett.* 23, 1829–1832.
- Sipkin, S.A., 1994. Rapid determination of global moment-tensor solutions. *Geophys. Res. Lett.* 21, 1667–1670.
- Sipkin, S.A., Jordan, T.H., 1975. Lateral heterogeneity of the upper mantle determined from the travel times of ScS. *J. Geophys. Res.* 80, 1474–1484.
- Sipkin, S.A., Jordan, T.H., 1976. Lateral heterogeneity of the upper mantle determined from the travel times of multiple ScS. *J. Geophys. Res.* 81, 6307–6320.
- Spakman, W., Nolet, G., 1988. Imaging algorithms, accuracy and resolution in delay time tomography. In: Vlaar, N.J., Nolet, G., Wortel, M., Cloetingh, S. (Eds.), *Mathematical Geophysics: A Survey of Recent Developments in Seismology and Geodynamics*. Reidel, Dordrecht, The Netherlands, pp. 155–187.
- Storey, B.C., 1995. The role of mantle plumes in continental breakup: case histories from Gondwanaland. *Nature* 377, 301–308.
- Strong, D., Stevens, R., 1974. Possible thermal explanation of contrasting Archean and Proterozoic geological regime. *Nature* 249, 545–546.
- Su, W.-j., Woodward, R., Diewonski, A.M., 1994. Degree-12 model of shear velocity heterogeneity in the mantle. *J. Geophys. Res.* 99, 6945–6980.
- Toksöz, M.N., Anderson, D.L., 1966. Phase velocities of long-period surface waves and structure of the upper mantle: I. Great-circle Love and Rayleigh wave data. *J. Geophys. Res.* 71, 1649–1658.
- Trampert, J., Woodhouse, J.H., 1995. Global phase-velocity maps of Love and Rayleigh-waves between 40 and 150 seconds. *Geophys. J. Int.* 122, 675–690.
- Trampert, J., Woodhouse, J.H., 1996. High resolution global phase velocity distributions. *Geophys. Res. Lett.* 23, 21–24.
- van der Hilst, R.D., Kennett, B.L.N., Christie, D., Grant, J., 1994. Project SKIPPY explores the lithosphere and mantle beneath Australia. *EOS Trans. Am. Geophys. Union* 75, 177–181.
- van der Hilst, R.D., Kennett, B.L.N., Shibutani, T., 1998. Upper mantle structure beneath Australia from portable array deployments. In: Braun, J., Dooley, J., Goleby, B., van der Hilst, R.D., Klootwijk, C. (Eds.), *Structure and Evolution of the Australian Continent*. AGU Geodynamics Series, AGU, Washington, DC, pp. 39–57.
- van der Lee, S., Nolet, G., 1997a. Seismic image of the subducted trailing fragments of the Farallon plate. *Nature* 386, 266–269.
- van der Lee, S., Nolet, G., 1997b. Upper mantle S-velocity structure of North America. *J. Geophys. Res.* 102, 22815–22838.
- Veevers, J.J. (Ed.), 1984. *Phanerozoic Earth History of Australia*. Oxford Univ. Press, Oxford, UK.

- Wang, Z., Dahlen, F.A., 1995. Validity of surface-wave ray theory on a laterally heterogeneous Earth. *Geophys. J. Int.* 123, 757–773.
- Wellman, P., 1998. Mapping of geophysical domains in the Australian continental crust using gravity and magnetic anomalies. In: Braun, J., Dooley, J., Goleby, B., van der Hilst, R.D., Klootwijk, C. (Eds.), *Structure and Evolution of the Australian Continent*. AGU Geodynamics Series, AGU, Washington, DC, pp. 59–71.
- Woodhouse, J.H., 1974. Surface waves in a laterally varying layered structure. *Geophys. J. R. Astron. Soc.* 37, 461–490.
- Woodhouse, J.H., Dziewonski, A.M., 1984. Mapping the upper mantle: Three-dimensional modeling of Earth structure by inversion of seismic waveforms. *J. Geophys. Res.* 89, 5953–5986.
- Zielhuis, A., 1992. *S-wave velocity below Europe from delay-time and waveform inversions*. PhD thesis, Utrecht Univ., Utrecht, The Netherlands.
- Zielhuis, A., Nolet, G., 1994a. Shear-wave velocity variations in the upper mantle beneath central Europe. *Geophys. J. Int.* 117, 695–715.
- Zielhuis, A., Nolet, G., 1994b. Deep seismic expression of an ancient plate boundary in Europe. *Science* 265, 79–81.
- Zielhuis, A., van der Hilst, R.D., 1996. Upper-mantle shear velocity beneath eastern Australia from inversion of waveforms from SKIPPY portable arrays. *Geophys. J. Int.* 127, 1–16.
- Zuber, M.T., Bechtel, T.D., Forsyth, D.W., 1989. Effective elastic thicknesses of the lithosphere and mechanisms of isostatic compensation in Australia. *J. Geophys. Res.* 94, 9353–9367.